

Strikingly Different Reactivity Patterns of Fischer Alkoxycarbene and Thiocarbene Complexes in Experimental and Theoretical Studies[†]

Betül Karatas, Isabella Hyla-Kryspin,[‡] and Rudolf Aumann*

Organisch-Chemisches Institut der Universität Münster, Corrensstrasse 40, 48149 Münster, Germany

Received April 23, 2007

Striking differences in the reactions of alkoxycarbene and thiocarbene complexes of chromium and tungsten are observed. Thus, (β -imino)ethoxycarbene complexes **10a–e**, generated in situ from [(OC)₅W=C(OEt)CH₂R] (**7a–c**; R = *n*-Pr, Me, *c*-C₇H₇) and imidoyl chlorides R¹ClC=NCHR²R³ (**9a–f**; R¹ = *t*-Bu, Ph, 2-furyl; R² = H, Me; R³ = Me, Et, Ph), undergo a metalla(di- π -methane) rearrangement to (*N*-enamino)ethoxycarbene complexes **12a–e**, while the corresponding (β -imino)thiocarbene complexes **11a–l**, derived from [(OC)₅M=C(SEt)CH₂R] (**8a–e**; M = W, Cr; R = *n*-Pr, Me, *c*-C₇H₇, *c*-C₆H₇Fe(CO)₃) and imidoyl chlorides under similar conditions, form pyrroles **16a–h** and **17k,l** by α -cyclization. On the basis of the calculated DFT/BP86 potential energy surfaces of the particular reaction channels it is shown that (β -imino)alkoxycarbene compounds **10** prefer a metalla(di- π -methane) rearrangement due to the kinetic stability of the (*N*-enamino)ethoxycarbene products, while formation of pyrroles is not favored due to the presence of high energetic stationary structures in the α -cyclization pathway. For (β -imino)thiocarbene compounds **11**, on the other hand, rearranged products are kinetically unstable, and α -cyclization reactions are strongly favored on thermodynamic grounds.

Introduction

Fischer alkoxycarbene and aminocarbene complexes¹ are widely applied in organic synthesis,² whereas the isostructural thiocarbene complexes have found little attention in this respect.³

(Alkyl)thiocarbene complexes [(OC)₅M=C(SR)alkyl] (M = Cr, W; R = Me, Et, Ph) are readily available by thiolysis of the corresponding (alkyl)alkoxycarbene complexes.^{4,5a,b,6b} An

efficient way to (aryl)thiocarbene complexes involves acetylation and thiolysis of the corresponding carbonylmetalates, e.g., [(OC)₅M(COC₆H₅)] [NMe₄] (M = Cr, W, Mn).^{6a,7} Thiolysis of (aryl)aminocarbene complexes is unfavorable on thermodynamic grounds, but is achieved after *N*-acylation.^{5c}

Reactions of (alkyl)thiocarbene complexes studied so far, include addition of phosphines,⁸ isocyanides,^{6b,c} alkynes,^{6d,7} and hydrogen bromide,⁹ condensation with aromatic aldehydes,^{6b} and insertion into carbon–hydrogen and metal–carbene bonds.¹⁰ Reactions of dithiocarbene complexes¹¹ and η^2 -thiocarbene complexes^{12,13} with amines, alkyl phosphines, and azides have also been reported, as well as the addition of hydrides and thiolates,¹⁴ alkyl- and arylsulfonium salts,¹³ trifluoroacetic acid,¹⁵ and thiocyanate salts.¹⁶

On the basis of the present knowledge, it appears that the reactions of thiocarbene complexes would follow the patterns

(5) (a) Raubenheimer, H. G.; Kruger, G. J.; Lombard, A.; Linford, L.; Viljoen, J. C. *Organometallics* **1985**, *4*, 275–284. (b) Raubenheimer, H. G.; Kruger, G. J.; Marais, C. F.; Otte, R.; Hattingh, J. T. Z. *Organometallics* **1988**, *7*, 1853–1858. (c) Raubenheimer, H. G.; Kruger, G. J.; Viljoen, H. W. *J. Chem. Soc., Dalton Trans.* **1985**, 1963–1966.

(6) (a) Aumann, R.; Schröder, J. *J. Organomet. Chem.* **1989**, *378*, 57–65. (b) Aumann, R.; Schröder, J. *Chem. Ber.* **1990**, *123*, 2053–2058. (c) Aumann, R.; Schröder, J.; Krüger, C.; Goddard, R. *J. Organomet. Chem.* **1989**, *378*, 185–197. (d) Aumann, R.; Schröder, J.; Heinen, H. *Chem. Ber.* **1990**, *123*, 1369–1374.

(7) Dötz, K. H.; Leue, V. *J. Organomet. Chem.* **1991**, *407*, 337–351. (8) Kreissl, F. R.; Fischer, E. O.; Kreiter, C. G.; Fischer, H. *Chem. Ber.* **1973**, *106*, 1262–1276.

(9) Fischer, E. O.; Kreis, G. *Chem. Ber.* **1973**, *106*, 2310–2314.

(10) (a) Raubenheimer, H. G.; Kruger, G. J.; Marais, C. F.; Otte, R.; Scott, F. S. *Afr. J. Chem.* **1987**, *40*, 207–208. (b) Raubenheimer, H. G.; Kruger, G. J.; Linford, L.; Marais, C. F.; Otte, R.; Hattingh, J. T. Z.; Lombard, A. *J. Chem. Soc., Dalton Trans.* **1989**, 1565–1577. (c) Raubenheimer, H. G.; Kruger, G. J.; Scott, F.; Otte, R. *Organometallics* **1987**, *6*, 1789–1795.

(11) (a) Pickering, R. A.; Jacobson, R. A.; Angelici, R. J. *J. Am. Chem. Soc.* **1981**, *103*, 817–821. (b) Pickering, R. A.; Angelici, R. J. *Inorg. Chem.* **1981**, *20*, 2977–2983.

* Corresponding author. E-mail: aumannr@uni-muenster.de.

[†] Organic Synthesis via Transition Metal Complexes, Part 122. For Part 121 see ref 17.

[‡] Theoretical calculations.

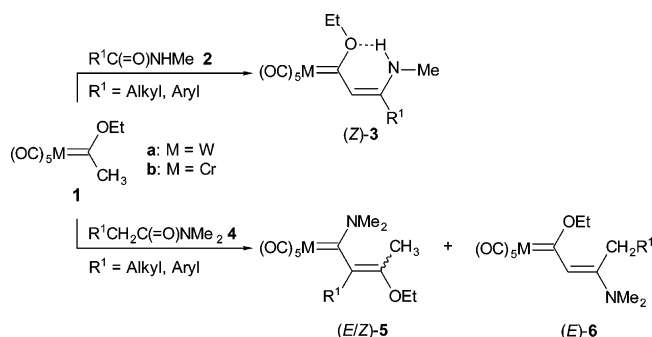
(1) Fischer, E. O.; Maasböl, A. *Angew. Chem.* **1964**, *76*, 645; *Angew. Chem., Int. Ed. Engl.* **1964**, *3*, 580.

(2) (a) Dötz, K. H. *Angew. Chem.* **1984**, *96*, 573–594; *Angew. Chem., Int. Ed. Engl.* **1984**, *23*, 587–608. (b) Wulff, W. D. In *Comprehensive Organic Synthesis*; Trost, B. M.; Fleming, I., Eds.; Pergamon: New York, 1991; Vol. 5, pp 1065–1113. (c) Wulff, W. D. In *Comprehensive Organometallic Chemistry II*; Abel, E. W., Stone, F. G. A., Wilkinson, G., Eds.; Pergamon: New York, 1995; Vol. 12, pp 469–547. (d) Doyle, M. D. In *Comprehensive Organometallic Chemistry II*; Abel, E. W., Stone, F. G. A., Wilkinson, G., Eds.; Pergamon: New York, 1995; Vol. 12, pp 387–420. (e) Wulff, W. D. In *Advances in Metal-Organic Chemistry*; Liebeskind, L. S., Ed.; JAI Press: Greenwich, CT, 1989; Vol. 1. (f) Harvey, D. F.; Sigano, D. M. *Chem. Rev.* **1996**, *96*, 271–288. (g) Frühauf, H.-W. *Chem. Rev.* **1997**, *97*, 523–596. (h) de Meijere, A.; Schirmer, H.; Duetsch, M. *Angew. Chem.* **2000**, *112*, 4124–4162; *Angew. Chem., Int. Ed.* **2000**, *39*, 3964–4002. (i) Dötz, K. H. *Pure Appl. Chem.* **1983**, *55*, 1689–1706. (j) Wu, Y.-T.; Kurahashi, T.; de Meijere, A. *J. Organomet. Chem.* **2005**, *690*, 5900–5911. (k) Barluenga, J.; Rodriguez, F.; Fananas, J. F.; Florez, J. *Top. Organomet. Chem.* **2004**, *13*, 59–121. (l) Gomez-Gallego, M.; Mancheno, M. J.; Sierra, M. A. *Acc. Chem. Res.* **2005**, *38*, 44–53. (m) Barluenga, J. *Pure Appl. Chem.* **2002**, *74*, 1317–1325. (n) Rudler, H.; Parlier, A. *Trends Organomet. Chem.* **1999**, *3*, 113–164. (o) Schwindt, M. A.; Miller, J. R.; Hegedus, L. S. *J. Organomet. Chem.* **1991**, *413*, 143–153. (p) Grotjahn, D. B.; Dötz, K. H. *Synlett* **1991**, *6*, 381–390. (q) Hegedus, L. S. *Pure Appl. Chem.* **1990**, *62*, 691–698.

(3) (a) Linford, L.; Raubenheimer, H. G. *Adv. Organomet. Chem.* **1991**, *32*, 1–119. (b) Linford, L.; Raubenheimer, H. G. *Comments Inorg. Chem.* **1991**, *12*, 113–138.

(4) Fischer, E. O.; Kreiter, C. G.; Müller, J.; Leupold, M. *Chem. Ber.* **1972**, *105*, 150–161.

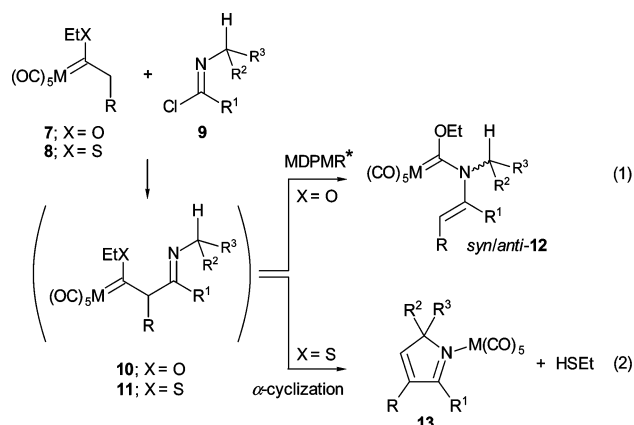
Scheme 1. Competition of Condensation and Insertion on Reactions of (Methyl)ethoxycarbene Complexes 1a,b with Secondary Amides 2 and Tertiary Amides 4, Respectively, in the Presence of POCl₃/NEt₃¹⁸



unrevealed for isostructural alkoxy carbene complexes. Fundamental differences in reactivities of thiocarbene and alkoxy carbene complexes were found only recently in condensation reactions of (alkyl)ethoxycarbene and (alkyl)thiocarbene complexes with acid amides.¹⁷

Reactions of (alkyl)ethoxycarbene complexes with imidoyl chlorides, generated in situ from acid amides and POCl₃/NEt₃, were shown to form condensation,^{18a,b} insertion,^{18c} and rearrangement products,^{18b} depending on the alkyl substituent of the (alkyl)ethoxycarbene complexes and the type of acid amide involved. Thus, for example β -(NH-amino)alkenylcarbene complexes [(OC)₅M=C(OEt)CH=C(NHMe)R¹], (*Z*)-**3**, were obtained as the only products from condensation of (methyl)ethoxycarbene complexes [(OC)₅M=C(OEt)CH₃] (**1a,b**; M = Cr, W) with secondary amides R¹C(=O)NHMe (**2**; R¹ = alkyl, aryl) in the presence of POCl₃/NEt₃ (Scheme 1),^{18a,b} whereas only small amounts of condensation products [(OC)₅M=C(OEt)CH=C(CH₂R¹)NMe₂], (*E*)-**6**,^{18c} but mainly insertion products [(OC)₅M=C(NMe₂)R¹C=C(OEt)CH₃], (*E/Z*)-**5**, were generated on condensation of (methyl)ethoxycarbene complexes with tertiary amides R¹CH₂C(=O)NMe₂ (**4**; R¹ = alkyl, aryl). On the other hand, reactions of (alkyl)ethoxycarbene complexes other than (methyl)ethoxycarbene compounds **1**, e.g., the (*n*-butyl)ethoxycarbene complex [(OC)₅W=C(OEt)*n*-Bu] (**7a**), and secondary amides **2** in the presence of POCl₃/NEt₃ gave (*N*-enamino)ethoxycarbene complexes **12** by a metalla(*di*- π -methane) rearrangement (Scheme 2, path 1).^{18b,19}

Scheme 2. Formation of (*N*-Enamino)ethoxycarbene Complexes 12a–e by a Metalla(*di*- π -methane) Rearrangement of (β -Imino)ethoxycarbene Complexes 10, and 2*H*-Pyrrole Complexes 13a–1 by α -Cyclization of (β -Imino)thiocarbene Complexes 11



*MDPMR = Metalla(*di*- π -methane) rearrangement

7,8M	R	10,12	M	X	R	R ¹	R ²	R ³	12 ^[a]	12 ^[b]	
a	W	<i>n</i> -Pr	a	W	O	<i>n</i> -Pr	<i>t</i> -Bu	H	Me	82	5/2
b	W	Me	b	W	O	Me	<i>t</i> -Bu	H	Me	68	3/1
c	W		c	W	O		Ph	H	Me	70	10/9
d	W		d	W	O	<i>n</i> -Pr	Ph	H	Me	71	2/1
e	Cr	<i>n</i> -Pr	e	W	O	Me	<i>t</i> -Bu	Me	Me	61	-/1

9	R ¹	R ²	R ³	11,13, 15–17 ^[c] M	X	R	R ¹	R ²	R ³	16 ^[c,d]	
a	<i>t</i> -Bu	H	Me	a	W	S	<i>n</i> -Pr	Ph	H	Et	78
b	Ph	H	Me	b	W	S	<i>n</i> -Pr	Ph	H	Ph	70
c	<i>t</i> -Bu	Me	Me	c	W	S	<i>n</i> -Pr	2-Furyl	H	Et	51
d	Ph	H	Et	d	W	S	<i>n</i> -Pr	<i>t</i> -Bu	H	Me	80
e	Ph	H	Ph	e	W	S	<i>n</i> -Pr	Ph	H	Me	71
f	2-Furyl	H	Et	f	W	S	Me	<i>t</i> -Bu	H	Me	75
g				g	W	S		Ph	H	Me	71
h				h	W	S		Ph	H	Me	64
i				i	Cr	S	<i>n</i> -Pr	<i>t</i> -Bu	H	Me	82
j				j	Cr	S	<i>n</i> -Pr	Ph	H	Me	72
k				k	W	S	<i>n</i> -Pr	<i>t</i> -Bu	Me	Me	- ^[e]
l				l	W	S	Me	<i>t</i> -Bu	Me	Me	- ^[e]

^aIsolated chemical yields in [%] of compounds **12**. ^b*syn/anti* ratio of isomers **12** according to ¹H NMR measurements. ^cFor the structures of compounds **15–17** see Scheme 3. ^dIsolated chemical yields of pyrroles **16** obtained by spontaneous transformation of pyrrole complexes **13**. Note that compounds **16c**, **16i**, **16e**, and **16j** are identical, although they were generated from different starting compounds. ^e1*H*-pyrroles **16** were not obtained in this case, but 2*H*-pyrroles **13k,l** and **17k,l** (Scheme 3) were identified by NMR measurements.

We now report on a quite unexpected strong influence of the heteroatoms oxygen and sulfur on the reactions of (alkyl)-heterocarbene complexes [(OC)₅M=CXCH₂R] **7a–c** (M = W; X = OEt) and **8a–e** (M = W, Cr; X = SEt), respectively, with imidoyl chlorides R¹CIC=NCHR²R³ **9a–f**, generated from secondary amides R¹C(=O)NHCHR²R³ **20** (Scheme 2).

Results and Discussion

Even though on first sight it might be expected that isostructural alkoxy carbene and thiocarbene complexes would react similarly, we found completely different reaction patterns for these compounds under certain circumstances. For example,

(20) Nerdel, F.; Weyerstahl, P.; Dahl, R. *Liebigs Ann. Chem.* **1968**, 716, 127–134.

(12) (a) Kim, H. P.; Kim, S.; Jacobson, R. A.; Angelici, R. J. *Organometallics* **1986**, 5, 2481–2488. (b) Kim, H. P.; Angelici, R. J. *Organometallics* **1986**, 5, 2489–2496. (c) Ullrich, N.; Keller, H.; Stegmair, C.; Kreissl, F. R. *J. Organomet. Chem.* **1989**, 378, C19–C22. (d) Schütt, W.; Herdtweck, E.; Kreissl, F. R. *J. Organomet. Chem.* **1993**, 456, C15–C17. (e) Ogric, C.; Schütt, W.; Lehotkay, T.; Herdtweck, E.; Kreissl, F. R. *Z. Naturforsch., B: Chem. Sci.* **1995**, 50, 1839–1844. (f) Ogric, C.; Lehotkay, T.; Wurst, K.; Jaitner, P.; Kreissl, F. R. *J. Organomet. Chem.* **1997**, 541, 71–75. (g) Ullrich, N.; Stegmair, C.; Keller, H.; Herdtweck, E.; Kreissl, F. R. *Z. Naturforsch., B: Chem. Sci.* **1990**, 45, 921–925.

(13) Ostermeier, J.; Schütt, W.; Stegmair, C. M.; Ullrich, N.; Kreissl, F. R. *J. Organomet. Chem.* **1994**, 464, 77–81.

(14) (a) Doyle, R. A.; Angelici, R. J. *Organometallics* **1989**, 8, 2207–2214. (b) Doyle, R. A.; Angelici, R. J. *J. Organomet. Chem.* **1989**, 375, 73–84.

(15) Kreissl, F. R.; Müller, F. X.; Wilkinson, D. L.; Müller, G. *Chem. Ber.* **1989**, 122, 289–290.

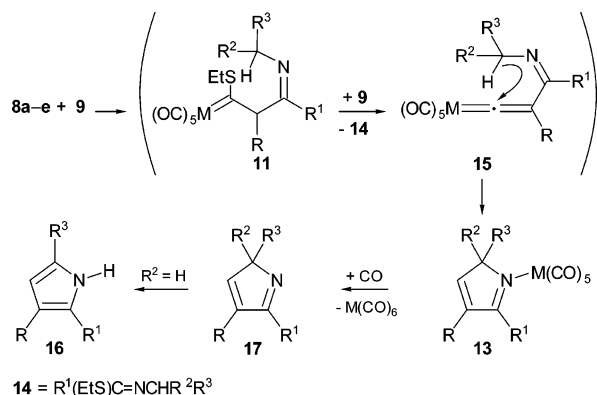
(16) Ogric, C.; Ostermeier, J.; Heckel, M.; Hiller, W.; Kreissl, F. R. *Inorg. Chim. Acta* **1994**, 222, 77–84.

(17) Nitsche, F.; Aumann, R.; Fröhlich, R. *J. Organomet. Chem.* **2007**, 692, 2971–2989.

(18) (a) Aumann, R.; Hinterding, P. *Chem. Ber.* **1990**, 123, 2047–2051. (b) Aumann, R.; Fu, X.; Vogt, D.; Fröhlich, R.; Kataeva, O. *Organometallics* **2002**, 21, 2736–2742. (c) Aumann, R.; Hinterding, P. *Chem. Ber.* **1990**, 123, 611–620.

(19) Ünalidi, S.; Aumann, R.; Fröhlich, R. *Chem.—Eur. J.* **2003**, 9, 3300–3309.

Scheme 3. Formation of 1*H*-Pyrroles 16, 2*H*-Pyrroles 17, and 2*H*-Pyrrole Complexes 13 from (β -Imino)thiocarbene Complexes 11 (for the numerical designation of compounds 15–17 see table of Scheme 2)



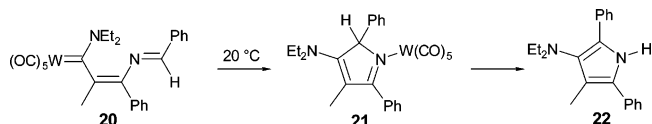
(alkyl)ethoxycarbene complexes **7a–c** afforded (*N*-enamino)-ethoxycarbene complexes **12a–e** on reaction with imidoyl chlorides **9** and triethylamine in 61–82% isolated yields, whereas the isostructural (alkyl)thiocarbene complexes **8a–e** did not give (*N*-enamino)thiocarbene complexes under these conditions, but formed 2*H*-pyrrole complexes **13a–l** instead (Scheme 2).

Common to both reaction paths (Scheme 2, paths 1 and 2) is the initial formation of (β -imino)heterocarbene complexes **10a–e** ($X = \text{O}$) and **11a–l** ($X = \text{S}$), respectively, which play a key role, since their reactions are strongly directed by the heteroatom. Thus (β -imino)ethoxycarbene complexes were found to undergo a spontaneous rearrangement to (*N*-enamino)-ethoxycarbene complexes **12a–e**,¹⁹ whereas (β -imino)thiocarbene complexes **11a–l** derived from (alkyl)thiocarbene complexes **8a–e** underwent an α -cyclization to pyrroles **16a–h**, via initial formation of thermolabile 2*H*-pyrrole complexes **13a–h** and 2*H*-pyrroles **17a–h** (Scheme 3).²¹ Other than the 2*H*-pyrrole complexes **13a–h** and 2*H*-pyrroles **17a–h**, the 2*H*-pyrrole complexes **13k,l** are reasonably stable due to the absence of an α -proton and, therefore, could be identified by NMR measurements in product mixtures with its demetalation compounds **17k,l**. The thiols, which are eliminated in this reaction, are captured by imidoyl chlorides **9a–f** to give thioesters $\text{R}^1\text{-(EtS)C}=\text{NCHR}^2\text{R}^3$ **14**.

A variety of 1*H*- and 2*H*-pyrroles were thus obtained from (alkyl)thiocarbene complexes **8a–e** and imidoyl chlorides **9a–f** in 51–82% isolated yields (Scheme 2).

The different reaction paths observed for ethoxycarbene compounds **7a–c** and thiocarbene compounds **8a–e** (Scheme

Scheme 5. Formation of 2*H*-Pyrrole Complex 21 and 1*H*-Pyrrole 22 by π -Cyclization of the 5-Aza-1-tungsta-1,3,5-hexatriene 20^{21b}

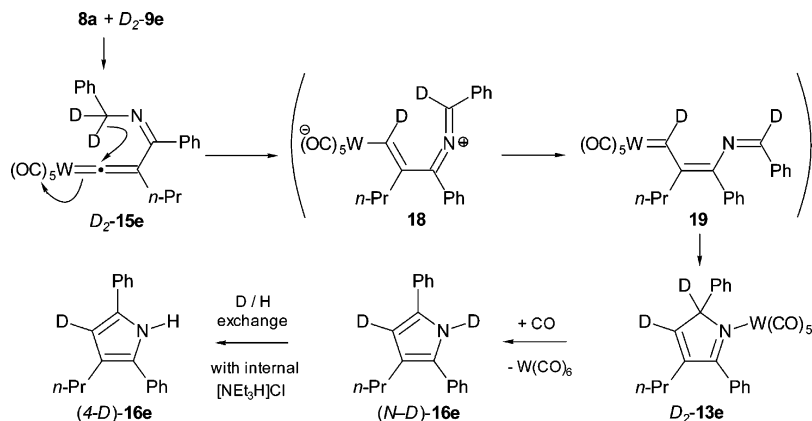


2, paths 1 and 2) are explained on the basis of multistep processes following the initial formation of (β -imino)heterocarbene complexes **10a–e** ($X = \text{O}$) and **11a–l** ($X = \text{S}$). On the basis of calculations presented below, it appears that an associative reaction step involving the addition of the β -imino nitrogen atom to the carbene carbon atom is favored for the (β -imino)ethoxycarbene complexes **10a–e** over that of the corresponding (β -imino)thiocarbene complexes **11a–l**, whereas a dissociative process leading to vinylidenes **15** is energetically favored in the case of (β -imino)thiocarbene complexes **11a–l**. Formation of vinylidenes **15** by elimination of thiol from a (β -imino)thiocarbene complex was shown to be energetically more favorable than the elimination of an alcohol from a (β -imino)-alkoxy carbene complex. Transfer of an α -hydrogen atom from the $=\text{N}-\text{CH}$ group to the vinylidene unit of compounds **15** gives 5-aza-1-metalla-1,3,5-hexatrienes **19**, which subsequently undergo a π -cyclization to pyrrole complexes **13** (Scheme 4). The regiochemistry of the hydride transfer has been clarified by a labeling experiment, in which the 1*H*-pyrrole (**4D**)-**16e** was generated from the (*n*-butyl)thiocarbene complex $[(\text{OC})_5\text{W}=\text{C}(\text{SEt})n\text{-Bu}]$ (**8a**) and the deuterated imidoyl chloride $\text{PhClC}=\text{NCD}_2\text{Ph}$ (**D₂-9e**) (Scheme 4).

The assumption that the 5-aza-1-metallatriene **19** would undergo a π -cyclization is in agreement with the reported stepwise transformation of the 5-aza-1-tungsta-1,3,5-hexatriene $[(\text{OC})_5\text{W}=\text{C}(\text{NEt})_2-\text{CMe}=\text{C}(\text{Ph})\text{N}=\text{CHPh}]$ (**20**) to the 2*H*-pyrrole complex **21** and finally the 1*H*-pyrrole **22** (Scheme 5).^{21b}

DFT Calculations. In order to gain deeper insight into the reaction mechanisms depicted in Scheme 2 as well as to obtain an answer on the question of why the alkoxy carbene complexes **7** and the thiocarbene complexes **8** prefer different reaction paths, the metalla (*di*- π -methane) rearrangements, abbreviated below as MDPM rearrangement, and the α -cyclization reactions were investigated for both types of complexes with the help of DFT calculations. The calculations were carried out on model tungsten complexes, in which the ethyl group bound to the O/S atoms in the experimental molecules as well as the substituents R , R^1 , R^2 , and R^3 were replaced by methyl groups. We started our investigations by searching the stationary structures of the postulated reactants **10** ($X = \text{O}$) and **11** ($X = \text{S}$) (see Scheme

Scheme 4. Deuterium Labeling Experiment Leading to Selectively Labeled Pyrrole (4*D*)-16e



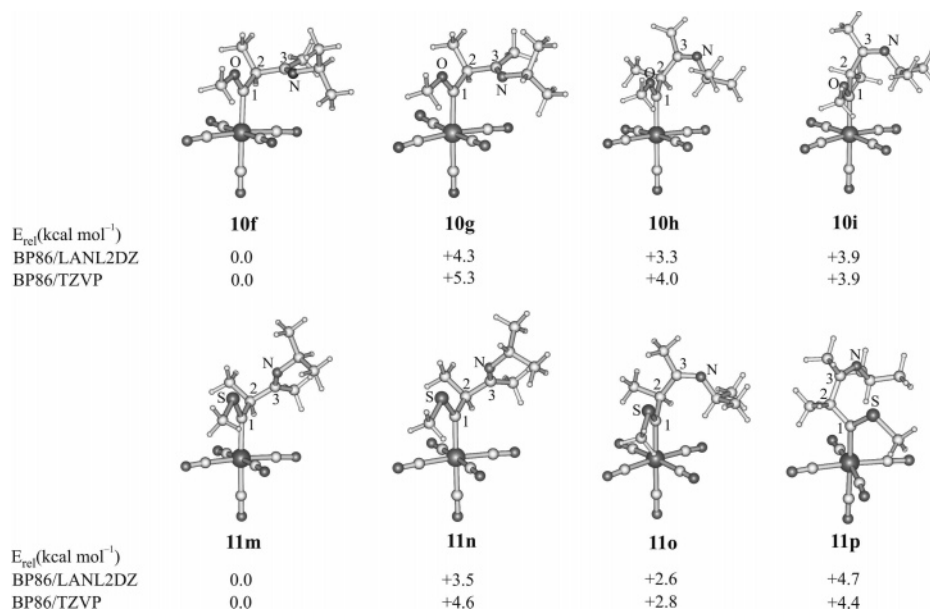


Figure 1. Optimized structures and relative electronic energies of the methoxy (**10f**–**10i**) and (methyl)thio (**11m**–**11p**) reactants.

2). Both types of reactants are characterized by large structural flexibility of the coordinated carbene ligand, and several stationary points were detected on their potential energy surfaces (Figure 1). From Figure 1 it is evident that the β -imino group of **10f**, **10g**, **11m**, and **11n** should be capable of approaching the carbene carbon atom easily and initiate the MDPM rearrangement, while **10h**, **10i**, **11o**, and **11p** may be regarded as starting structures for the α -cyclization reactions. The calculated reaction channels of the MDPM rearrangements and the α -cyclization reactions are discussed in the next sections in more detail.

MDPM Rearrangement of the Methoxy (10f**, **10g**) and the (Methyl)thio (**11m**, **11n**) Carbene Complexes.** The MDPM rearrangements proceed through four-membered cyclic structures of the carbene ligand, which independently of the basis set used for calculations were located as transition states (TS) of the reactions. For the sake of clarity they are labeled below as TS(**10f**→**12f**), TS(**10g**→**12g**), TS(**11m**→**12m**), and TS(**11n**→**12n**).

The molecular shapes of the optimized structures of transition states and products are shown in Figure 2. The corresponding potential energy profiles are depicted in Figures 3 and 4. Selected BP86/TZVP-optimized parameters of the relevant stationary structures as well as the analogous data from BP86/LANL2DZ calculations together with the number of imaginary frequencies are provided in the Supporting Information (Table S1, Table S2, Figure S1, and Figure S2).

Compared to the reactants **10f/11m** and **10g/11n**, the structural changes in the transition states TS(**10f**→**12f**)/TS(**11m**→**12m**) and TS(**10g**→**12g**)/TS(**11n**→**12n**) are clearly indicative of the C1–N bond formation and breakage of the C1–C2 bond. Thus, upon going from **10f/11m** to the transition states TS(**10f**→**12f**)/TS(**11m**→**12m**) the C1–C2 bond stretches by 0.078 Å/0.061 Å, the C2–C3–N bond angle diminishes by 21.6°/15.5°, and the C1–N distance shortens significantly by 1.155 Å/1.048 Å. All these changes are accompanied by elongation of the W–C1 and C1–O/S bonds by 0.204 Å/0.099 Å and 0.084 Å/0.073 Å, respectively. Compared to the TS(**10f**→**12f**)/TS(**11m**→**12m**) the C1–N bond formation and breakage of the C1–C2 bond are

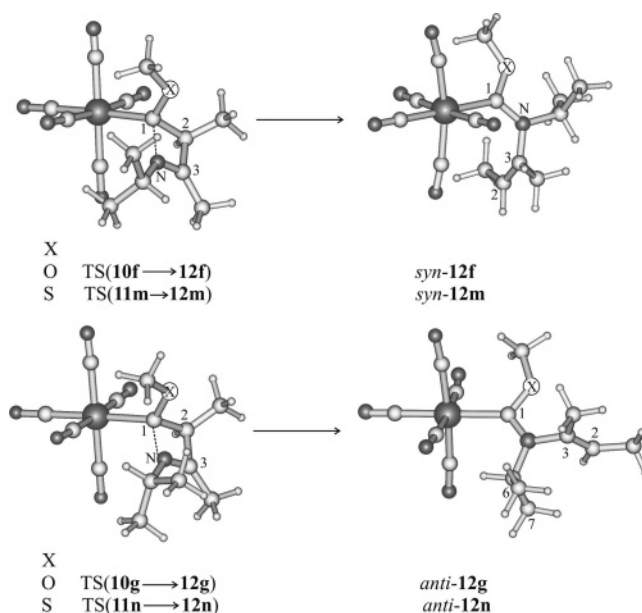


Figure 2. Molecular shapes of the optimized structures of transition states and products for the MDPM rearrangements of **10f/11m** → *syn*-**12f/syn-12m** and **10g/11n** → *anti*-**12g/anti-12n**.

less pronounced in the TS(**10g**→**12g**)/TS(**11n**→**12n**). With respect to the reactants **10g/11n**, the C1–N bond distance of the TS(**10g**→**12g**)/TS(**11n**→**12n**) is 0.902 Å/0.978 Å shorter and that of the C1–C2 bond 0.059 Å/0.056 Å longer; that is, these changes are smaller than in the case of **10f/11m** → **12f/12m** reactions.

The MDPM rearrangement **10f** → *syn*-**12f** is an exothermic process with a moderate reaction barrier. The product *syn*-**12f** is 5.7 kcal mol⁻¹ more stable than the reactant **10f**, and the reaction barrier amounts to 14.9 kcal mol⁻¹ (Figure 3, right side). The analogous reaction of the (methyl)thio complex, **11m** → *syn*-**12m**, is characterized by lower exothermicity and lower reaction barrier. The calculations predict a reaction barrier of 10.7 kcal mol⁻¹ and an exothermicity of only 1.7 kcal mol⁻¹ (Figure 4, right side). Thus, with respect to the reaction of the methoxy species, **10f** → *syn*-**12f**, the MDPM rearrangement of the (methyl)thio species, **11m** → *syn*-**12m**, is a thermodynamically

(21) (a) Aumann, R.; Heinen, H.; Krüger, C.; Betz, P. *Chem. Ber.* **1990**, *123*, 599–604. (b) Aumann, R.; Heinen, H.; Goddard, R.; Krüger, C. *Chem. Ber.* **1991**, *124*, 2587–2593. (c) Aumann, R.; Fröhlich, R.; Zippel, F. *Organometallics* **1997**, *16*, 2571–2580.

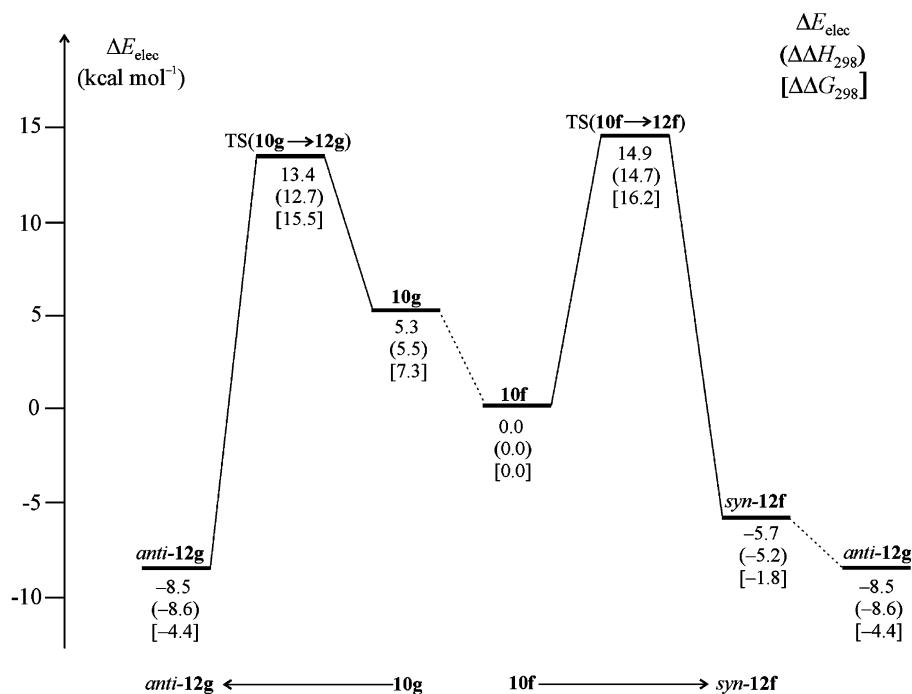


Figure 3. BP86/TZVP potential energy profiles for the MDPM rearrangement of the methoxy complexes **10f** and **10g**. The depicted energy levels refer to ΔE_{elec} , values in parentheses are relative enthalpies at 298 K ($\Delta\Delta H_{298}$), and those in square brackets are relative Gibbs free energies at 298 K ($\Delta\Delta G_{298}$).

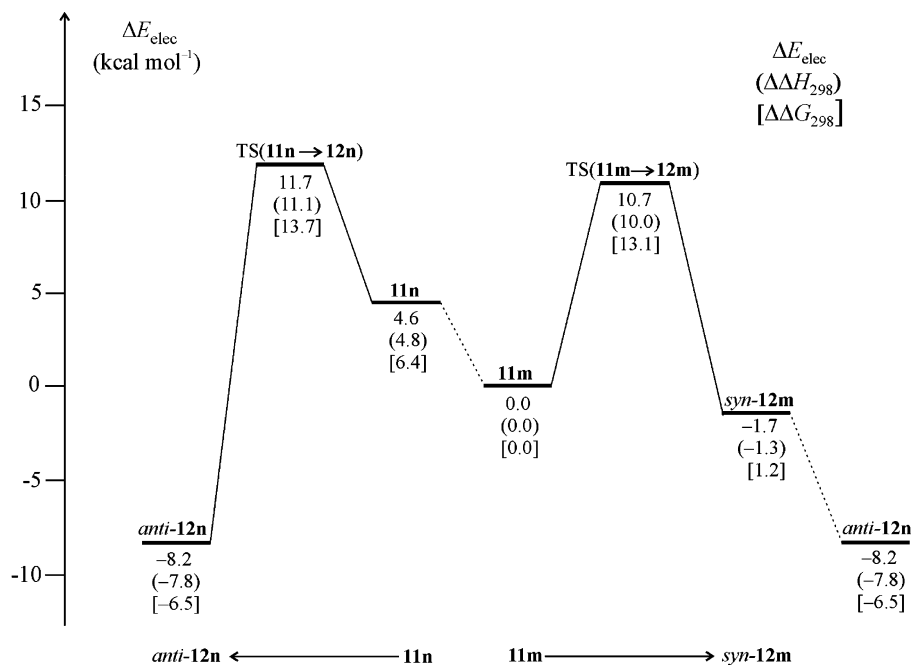


Figure 4. BP86/TZVP potential energy profiles for the MDPM rearrangement of the (methyl)thio complexes **11m** and **11n**. The depicted energy levels refer to ΔE_{elec} , values in parentheses are relative enthalpies at 298 K ($\Delta\Delta H_{298}$), and those in square brackets are relative Gibbs free energies at 298 K ($\Delta\Delta G_{298}$).

cally less favored reaction. Furthermore, due to the low-energy barrier of the reverse process $\text{syn-12m} \rightarrow \mathbf{11m}$ (12.4 kcal mol⁻¹) compared to that of the reverse $\text{syn-12f} \rightarrow \mathbf{10f}$ reaction (20.6 kcal mol⁻¹), the (methyl)thio product syn-12m is kinetically less stable than the methoxy syn-12f one.

Adding zero-point vibrational energy (ZPVE) and thermal corrections to the electronic energies ΔE_{elec} , that is, considering the relative enthalpies $\Delta\Delta H_{298}$, does not change these conclusions (Figures 3 and 4). Adding further entropy contributions, that is, considering the relative Gibbs free energies ($\Delta\Delta G_{298}$), increases the energy barriers, diminishes the exothermicity of

the MDPM reactions, and destabilizes **10g** and **11n** compared to the global minimum reactants **10f** and **11m** (Figures 3 and 4). The MDPM rearrangement of the (methyl)thio complex, $\mathbf{11m} \rightarrow \text{syn-12m}$, with a $\Delta\Delta G_{298}(\text{syn-12m})$ of 1.2 kcal mol⁻¹ is now a slightly endothermic reaction, and that of the methoxy complex, $\mathbf{10f} \rightarrow \text{syn-12f}$, with a $\Delta\Delta G_{298}(\text{syn-12f})$ of -1.8 kcal mol⁻¹ is still an exothermic process. However, the complexes syn-12f and syn-12m are not the lowest energy structure among the *N*-enamino products.

Lower energy products, that is, *anti-12g* and *anti-12n*, are found when the MDPM rearrangement begins with the reactants

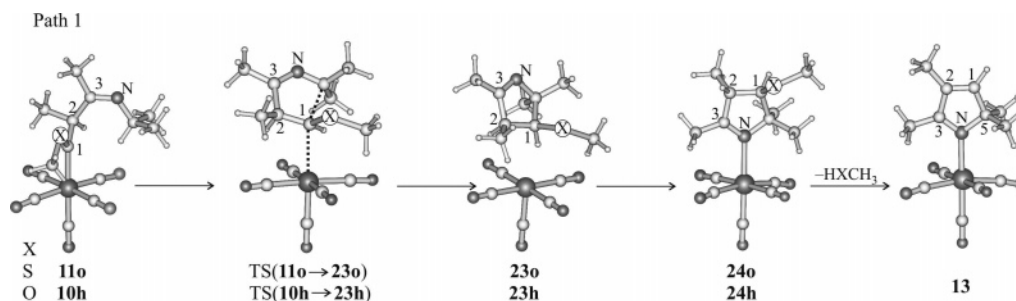


Figure 5. Molecular shapes of the optimized stationary structures of the (methyl)thio and methoxy species for α -cyclization reactions according to path 1.

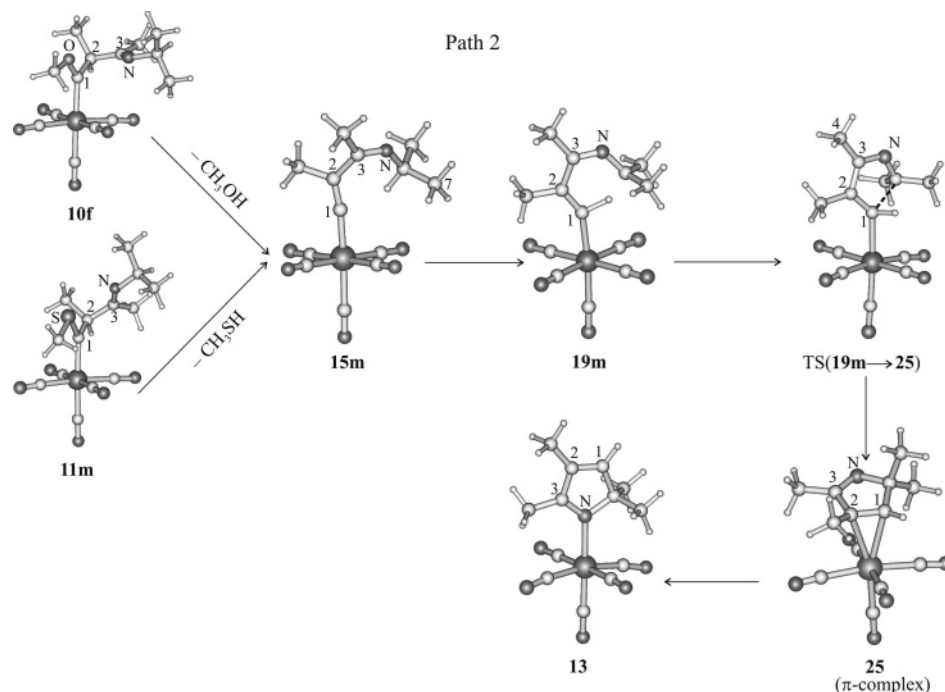


Figure 6. Molecular shapes of the optimized stationary structures for the α -cyclization reactions according to path 2.

10g and **11n** (Figures 3 and 4, left side). In terms of ΔE_{elec} *anti*-**12g** and *anti*-**12n** are 2.8 and 6.5 kcal mol⁻¹ more stable than *syn*-**12f** and *syn*-**12m**, respectively. The energy profiles for the formation of *N*-enamino products *anti*-**12g** and *anti*-**12n** from the reactants **10g** and **11n** are very similar (Figure 3 and 4, left side). The calculated reaction barriers ($\Delta E_{\text{elec}}^{\ddagger}$) amount to 8.1 kcal mol⁻¹ for TS(**10g**→**12g**) and to 7.1 kcal mol⁻¹ for TS(**11n**→**12n**). The exothermicity (ΔE_{elec}) of the reaction **10g** → *anti*-**12g** (13.8 kcal mol⁻¹) is almost the same as that of the reaction **11n** → *anti*-**12n** (12.8 kcal mol⁻¹). These energetic differences are too small to account for the different behavior of the alkoxy and (alkyl)thio species. Moreover, **10g** and **11n**, with ΔE_{elec} of 5.3 and 4.6 kcal mol⁻¹ above **10f** and **11m**, are the less stable reactants. Thus, it is very likely that both species will not be involved in the reactions. Note that the *anti*-forms should also be attainable from the *syn*-products by rotation of the *N*-enamino part of the carbene ligand. These findings are in accord with the experimental evidence that (i) at the beginning of the MDPM rearrangement the formation of the alkoxy *syn*-products **12a–d** dominates the formation of the *anti*-**12a–d** ones, and (ii) as time passes, the *syn*-isomers slowly convert into the *anti*-forms.

Formation of Pyrrole Complexes 13 from the Methoxy (10h, 10f) and (Methyl)thio (11o, 11m) Carbene Complexes. In this section we focus on the comparison of possible reaction paths for the formation of pyrrole complexes **13**. Since in these

processes the elimination of ethanethiol and the formation of thioesters may occur either prior or after the ring closure, we decided to explore the potential energy surfaces (PES) of the corresponding reaction paths of these α -cyclization reactions. In path 1 we assume that the reactions begin with the model reactants **11o** and **10h** (Figure 5). The hydride migration and ring closure yield the adducts **23o** and **23h**, which rearrange to complexes **24o** and **24h**. The elimination of methanethiol/methanol from **24o/24h** takes place in the last step of the reactions, and the *2H*-pyrrole complex **13** is produced.

In path 2, we begin the reactions with the global minimum reactants **11m** and **10f**. The elimination of methanethiol/methanol takes place at the early stage of the reactions, giving the vinylidene **15m** (Figure 6). The hydride migration in **15m** yields the hexatriene **19m** and is followed by the ring closure. The resulting π -complex **25** rearranges then to the *2H*-pyrrole complex **13** (Figure 6).

The TS(**11o**→**23o**) and TS(**10h**→**23h**) of path 1 calculated with the TZVP basis set correspond to transition states for a simultaneous hydrogen transfer and ring closure (Figure 5). Both transition states are characterized by one strong imaginary mode reflecting the ring closure process {499.7i cm⁻¹ [TS(**11o**→**23o**)], 538.9i cm⁻¹ [TS(**10h**→**23h**)]}. All attempts to locate the stationary points for hydrogen transfer that is followed by the ring closure failed. The energy barrier ($\Delta E_{\text{elec}}^{\ddagger}$) for the reaction step **10h** → **23h** of the oxo species is 6.2 kcal mol⁻¹ higher

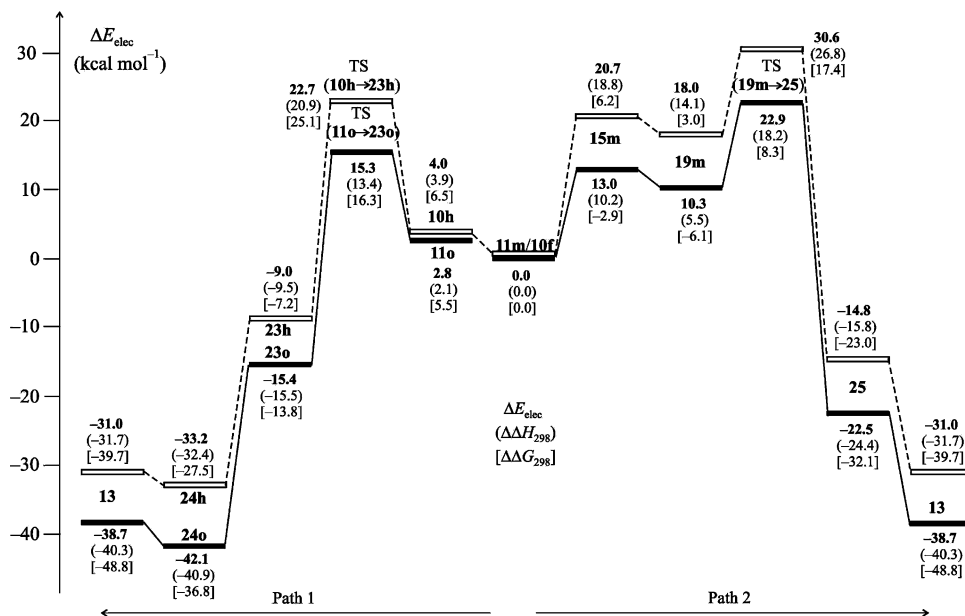


Figure 7. Potential energy profiles for α -cyclization reactions of the oxo (**10f**, **10h**) and the thio (**11m**, **11o**) carbene complexes according to path 1 (left) and path 2 (right). The depicted energy levels refer to relative electronic energies (ΔE_{elec}), which are given in bold. Values in parentheses are relative enthalpies at 298 K ($\Delta\Delta H_{298}$), and those in square brackets are relative Gibbs free energies at 298 K ($\Delta\Delta G_{298}$). The stationary points of the oxo complexes are connected by the dashed lines and those of the thio species by the solid lines.

than for the analogous reaction of the thio species, **11o** \rightarrow **23o** (Figure 7, left side). Including entropic effects ($\Delta\Delta G_{298}^\ddagger$) slightly increases this value to 8.5 kcal mol⁻¹.

In accordance with the saturated nature of the C1 and C2 carbon atoms of the cyclic ligand, the W–C1 and W–C2 distances of the adducts **23o** and **23h** are long [3.406, 3.926 Å (**23o**), 3.391, 3.967 Å (**23h**)] and the interaction energies with the W(CO)₅ fragment are very weak (below 2 kcal mol⁻¹). Thus, **23o** and **23h** should easily rearrange to the intermediates **24o** and **24h**. The ring closure and the complexation of the cyclic ligand are exothermic processes (Figure 7). In terms of ΔE_{elec} , the ring closure of the thio species, **11o** \rightarrow **23o**, is 5.2 kcal mol⁻¹ more exothermic than that of the oxo species **10h** \rightarrow **23h**. Compared with **23o** and **23h**, the formation of the W–N bond stabilizes **24o** and **24h** by a comparable amount of energy [26.7 kcal mol⁻¹ (**24o**), 24.2 kcal mol⁻¹ (**24h**)]. The last elementary step, that is, the elimination of methanethiol/methanol and formation of the pyrrole complex **13** (**24o/24h** \rightarrow **13**), proceeds uphill on the PES of ΔE_{elec} (Figure 7). With respect to **24o/24h** it is slightly endothermic by approximately the same amount of energy, that is, 3.4 kcal mol⁻¹ for **24o** \rightarrow **13** and 2.2 kcal mol⁻¹ for **24h** \rightarrow **13**. The elimination of methanethiol/methanol is almost thermoneutral on the PES of $\Delta\Delta H_{298}$, but due to the large entropic contributions it is exogenic on the PES of Gibbs free energies (–12.0 kcal mol⁻¹ for **24o** \rightarrow **13**, –12.2 kcal mol⁻¹ for **24h** \rightarrow **13**). The entropic contributions for the elimination processes **24o/24h** \rightarrow **13** are on the order of 8 kcal mol⁻¹. As should be expected for processes with a constant number of particles, the entropic contributions are less significant for the preceding reaction steps (2–5 kcal mol⁻¹).

From Figure 6 it is evident that the possible different behavior of the oxo and thio species reacting according to path 2 must be determined by the first elementary reaction step, that is, by the formation of the vinylidene complexes **15**. An examination of the PES calculated for path 2 of the α -cyclization reactions (Figure 6 and Figure 7, right side) shows that formation of the vinylidene **15m** is an endothermic process in terms of ΔE_{elec} and $\Delta\Delta H_{298}$. However, in this case here the elimination of methanethiol with a ΔE_{elec} (**11m** \rightarrow **15m**) of 13.0 kcal mol⁻¹ is

7.7 kcal mol⁻¹ less endothermic than that of methanol, for which the ΔE_{elec} (**10f** \rightarrow **15m**) amounts to 20.7 kcal mol⁻¹. On the PES of Gibbs free energies the elimination of methanethiol, with a $\Delta\Delta G_{298}$ (**11m** \rightarrow **15m**) of –2.9 kcal mol⁻¹, is now an exothermic reaction, while that of methanol, with a $\Delta\Delta G_{298}$ (**10f** \rightarrow **15m**) of 6.2 kcal mol⁻¹, is still an endothermic process.

It is clear that, with respect to the PES of the thio species, all subsequent reaction steps of the oxo species will be shifted uphill by the same amount of energy, that is, 7.7 kcal mol⁻¹ in terms of ΔE_{elec} and 9.1 kcal mol⁻¹ in terms of $\Delta\Delta G_{298}$. Thus, at this point we can conclude that with respect to the thio reactant **11m** the α -cyclization reaction of the oxoreactant **10f** is not favored on thermodynamical grounds.

In the second step of path 2 a barrierless hydrogen transfer in **15m** occurs and the hexatriene complex **19m** is produced. The corresponding potential energy profile is provided in the Supporting Information. The hydrogen transfer is a slightly exothermic process, –2.7 kcal mol⁻¹ in terms of ΔE_{elec} , –3.2 kcal mol⁻¹ in terms of $\Delta\Delta G_{298}$. The optimized parameters of **15m** and **19m** exhibit the expected features of the complexed vinylidene and hexatriene ligands. The TS(**19m** \rightarrow **25**) exhibits one strong imaginary frequency (604.3i cm⁻¹), which reflects the ring-closing process. In terms of $\Delta E_{\text{elec}}^\ddagger$ the TS(**19m** \rightarrow **25**) is 12.6 kcal mol⁻¹ above **19m**. Including entropic effects increases the reaction barrier ($\Delta\Delta G_{298}^\ddagger$) to 14.4 kcal mol⁻¹.

The ring closure process in the TS(**19m** \rightarrow **25**) is more advanced than in the TS(**11o** \rightarrow **23o**) or the TS(**10h** \rightarrow **23h**) of path 1. Compared with the TS(**11o** \rightarrow **23o**)/TS(**10h** \rightarrow **23h**), the newly formed C1–C bond in the TS(**19m** \rightarrow **25**) is 0.529 Å/0.496 Å shorter. The formation of the π -complex **25** and the subsequent rearrangement to the pyrrole **13** are exothermic processes. In terms of ΔE_{elec} the π -complex **25** lies 32.8 kcal mol⁻¹ below the hexatriene **19m** and pyrrole **13** is 16.2 kcal mol⁻¹ more stable than **25** (Figure 7).

If we now consider the energetics calculated for the particular steps of path 1 and path 2, we can conclude that the α -cyclization reactions of the thio species are kinetically and thermodynamically favored over the analogous reactions of the oxo species (Figure 7). From comparison of the relative energies

with respect to the most accessible reactants **11m** and **10f** it follows that for both reaction pathways the highest stationary points on the particular PESs correspond to the transition states for the ring-closing processes. On the PES of ΔE_{elec} and $\Delta\Delta H_{298}$ path 1 is favored over path 2, for both thio and oxo species. In terms of ΔE_{elec} the TS(**19m**→**25**) of path 2 are 7.6 and 7.9 kcal mol⁻¹ above TS(**11o**→**23o**) and TS(**10h**→**23h**) of path 1 of the thio and oxo species, respectively. However, considering entropic contributions changes this situation in favor of path 2. On the PES of $\Delta\Delta G_{298}$ TS(**19m**→**25**) are now 8.0 and 7.7 kcal mol⁻¹ below TS(**11o**→**23o**) and TS(**10h**→**23h**), respectively. Furthermore, **11o** and **10h**, with a $\Delta\Delta G_{298}$ of 5.5 and 6.5 kcal mol⁻¹ above **11m** and **10f**, respectively, are quite unfavorable for the beginning of α -cyclization reactions, and therefore we believe that path 1 is not relevant for the mechanism under study. Further support for path 2 comes also from the experimentally detected formation of the 1*H*-pyrrole **22** from the closely related 5-aza-1-tungsta-1,3,5-hexatriene complex **20** (Scheme 5).^{21b}

Summary and Conclusions

Remarkable reactivity differences of isostructural (alkyl)ethoxycarbene [(OC)₅W=C(OEt)CH₂R] (**7a–c**; R = *n*-Pr, Me, *c*-C₇H₇) and (alkyl)thiocarbene complexes [(OC)₅M=C(SEt)CH₂R] (**8a–e**; M = W, Cr; R = *n*-Pr, Me, *c*-C₇H₇, *c*-C₆H₇Fe(CO)₃) toward imidoyl chlorides R¹CIC=NCHR²R³ (**9a–f**; R¹ = *t*-Bu, Ph, 2-furyl; R² = H, Me; R³ = Me, Et, Ph) were found. The reaction of (alkyl)ethoxycarbene complexes **7a–c** with imidoyl chlorides in the presence of triethylamine afforded (*N*-enamino)ethoxycarbene complexes **12**, whereas (alkyl)thiocarbene complexes **8a–e** gave pyrroles **17** and **16**, respectively. The formation of compounds **12** was shown to involve a metalla(di- π -methane) skeletal rearrangement of the (β -imino)ethoxycarbene complexes **10a–e**, by which the C–C bond between the α -carbon atom and the carbene carbon atom is broken under the influence of the β -imino functionality. On the other hand, 1*H*- and 2*H*-pyrroles **16** and **17** were obtained by α -cyclization of the (β -imino)thiocarbene complexes **11a–l**.

The comparison of the calculated PESs for the preferred reaction pathways is depicted in Figure 8. As discussed in the previous sections, the first elementary step of both reaction channels begins with the lowest energy oxo (**10f**) and thio (**11m**) reactants. The MDPM rearrangements are facile one-step reactions that are due to an intramolecular associative process. The α -cyclization reactions proceed stepwise following the dissociative mechanism of the methanethiol/methanol elimination. From Figure 8 it is evident that the α -cyclization reaction of both the thio complex **11m** and the oxo complex **10f** is thermodynamically favored over the corresponding MDPM rearrangement. The overall exothermicity of the α -cyclization reactions with a $\Delta E_{\text{elec}}(\mathbf{13})$ of -31.0 kcal mol⁻¹ (X = O) and -38.7 kcal mol⁻¹ (X = S) is much larger than that of the MDPM rearrangements, for which ΔE_{elec} amounts to -5.7 kcal mol⁻¹ for *syn*-**12f** (X = O) and -1.7 kcal mol⁻¹ for *syn*-**12m** (X = S) (Figure 8, top). Thus, the different reactivity of the oxo and thio species should be due either to the kinetic factors or to the relative ease of the particular elementary steps.

The activation barriers of the MDPM rearrangements with a $\Delta E_{\text{elec}}^{\ddagger}$ of 14.9 kcal mol⁻¹ for TS(**10f**→**12f**) (X = O) and 10.7 kcal mol⁻¹ for TS(**11m**→**12m**) (X = S) do not differ much from the activation barrier of the ring-closing process of 12.6 kcal mol⁻¹ calculated for TS(**19m**→**25**) of the α -cyclization reaction. Considering entropic contributions slightly raises the activation barriers, but the differences between $\Delta\Delta G_{298}^{\ddagger}$ of TS(**10f**→**12f**)/TS(**11m**→**12m**) and TS(**19m**→**25**) are still in the

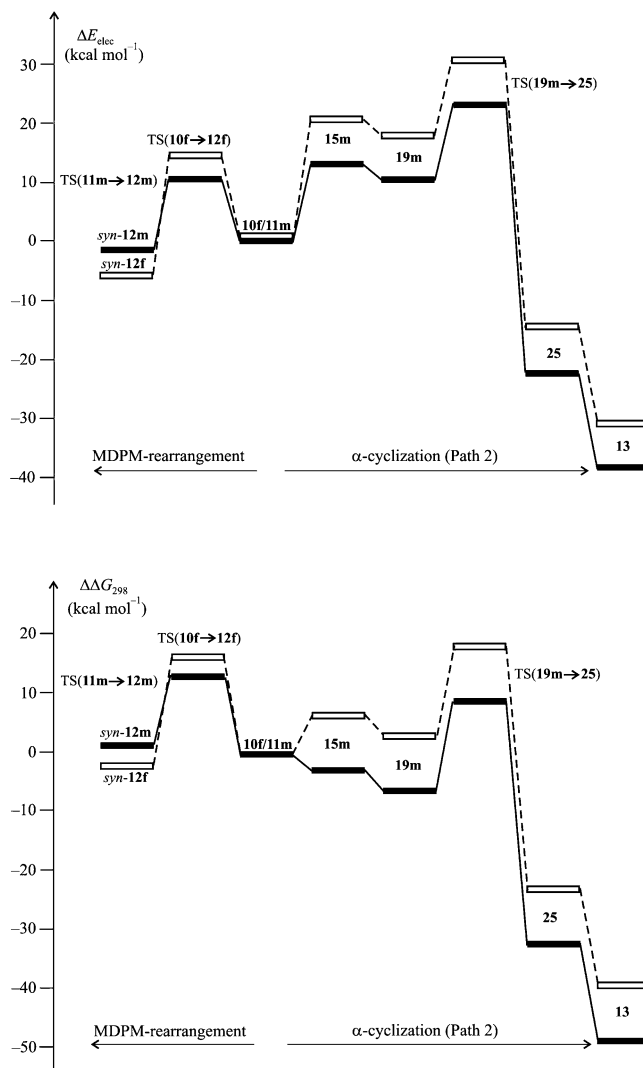


Figure 8. Potential energy surfaces of ΔE_{elec} (top) and $\Delta\Delta G_{298}$ (bottom) for the preferred reaction paths of the MDPM rearrangements and the α -cyclization reactions of the oxo (**10f**) and thio (**11m**) reactants. The stationary points of the oxo complexes are connected by the dashed lines and those of the thio species by the solid lines.

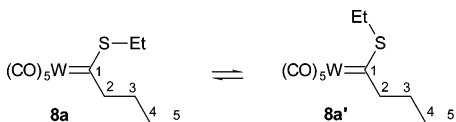
range of 2 kcal mol⁻¹ (Figure 8, bottom). These findings suggest comparable kinetic forces for the MDPM rearrangements **10f** → *syn*-**12f/11m** → *syn*-**12m** and the elementary ring-closing step **19m** → **25** of the α -cyclization reaction. However, taking into account the reaction barrier of the reverse processes *syn*-**12m** → **11m** ($\Delta\Delta G_{298}^{\ddagger} = 11.9$ kcal mol⁻¹) and *syn*-**12f** → **10f** ($\Delta\Delta G_{298}^{\ddagger} = 18.0$ kcal mol⁻¹) we can conclude that in addition to the above-discussed thermodynamical grounds the α -cyclization reaction of the thio complex **11m** is also favored because of the kinetic instability of the thio product *syn*-**12m** of the MDPM rearrangement. Furthermore, in terms of $\Delta\Delta G_{298}$, TS(**19m**→**25**) lies 8.3 kcal mol⁻¹ above the reactant **11m** and should be more easily accessible than that of the MDPM rearrangement [TS(**11m**→**12m**)], which is 13.1 kcal mol⁻¹ above **11m**. For the oxo complex **10f** the elimination of methanol requires more energy [$\Delta E_{\text{elec}}(\mathbf{15}) = 20.7$ kcal mol⁻¹] than the activation barrier for TS(**10f**→**12f**) of the MDPM rearrangement ($\Delta E_{\text{elec}}^{\ddagger} = 14.9$ kcal mol⁻¹) and TS(**19m**→**25**) of the α -cyclization reaction is 30.6 kcal mol⁻¹ above the reactant **10f** (Figure 8, top). Although entropic contributions stabilizes **15** with respect to TS(**10f**→**12f**), the elimination of methanol is still endothermic and the transition state of the α -cyclization

reaction is 1.2 kcal mol⁻¹ above that of the MDPM rearrangement (Figure 8 bottom). Thus, the MDPM rearrangement of the oxo reactant **10f** is a preferred reaction due to the kinetic stability of the *syn*-**12f** product, while the α -cyclization reaction is unfavorable due to the presence of high-energetic stationary states.

Experimental Section

All operations were carried out under an atmosphere of argon. ¹H and ¹³C NMR spectra were routinely recorded on Bruker ARX 300 and Bruker AMX 400 instruments. COSY, HMQC, HMBC, TOCSY, and NOE experiments were performed on Bruker AMX 400, Inova 500, and Varian Unity Plus 600 instruments. Chemical shifts δ were recorded against TMS as internal standards. IR spectra were recorded on a Biorad Digilab Division FTS-45 FT-IR spectrophotometer. Mass spectra were measured on a Finnigan Mat8200. Elemental analyses were determined on a Vario EL III elemental analyzer. All melting points reported are uncorrected. Analytical TLC plates (Merck DC-Alufolien Kieselgel 60F₂₄₀) were viewed by UV light (254 nm) and stained using iodine. *R_f* values refer to TLC tests. Chromatographic purification was performed on Merck Kieselgel 60. All reactions were performed under argon. The solvents were used as purchased and were not dried further. **7c**,^{22a} **7d**,^{22b} **9**,²⁰ and *N*-benzyl- α,α -*d*₂-benzamide²³ were prepared according to literature methods, and syntheses of the compounds **7a**,**b**,**e**^{22c} were achieved analogous to the synthesis of pentacarbonyl(1-methoxyethylidene)chromium.

Pentacarbonyl[1-(ethylthio)pentylidene]tungsten (8a). Pentacarbonyl(1-ethoxypentylidene)tungsten (**7a**) (876 mg, 2.00 mmol) in methanol (5 mL) was added to a stirred suspension of sodium carbonate (254 mg, 2.40 mmol) in methanol (20 mL) at -40 °C. After ca. 5 min, ethanethiol (248 mg, 4.00 mmol) in methanol (1 mL) was added dropwise to the yellow suspension. The reaction mixture was stirred for 1 h at -40 °C and then quenched by addition of a few drops of 85% phosphoric acid to give a red solution. Water (10 mL) was added and the product was extracted with *n*-pentane (3 × 50 mL). The combined organic layers were dried over MgSO₄ and then concentrated under reduced pressure to give a 13:2 mixture of **8a/8a'** (880 mg, 97%, *R_f* = 0.6 in *n*-pentane, red oil).



8a [8a']. ¹H NMR (400 MHz, CDCl₃, 25 °C): δ 3.80 [3.78] (dd, ³*J* = 8.4 and 7.5 Hz, 2H; 2-H₂), 2.99 [3.62] (q, ³*J* = 7.7 Hz, 2H; SCH₂), 1.66 [1.73] (m, 2H; 3-H₂), 1.55 [1.55] (m, 2H; 4-H₂), 1.36 [1.47] (t, ³*J* = 7.7 Hz, 3H; SCH₂CH₃), 1.01 [1.01] (t, ³*J* = 7.3 Hz, 3H; 5-H₃). ¹³C NMR (CDCl₃, 25 °C): δ 337.6 [345.2] (C_q, W=C), 206.7 and 197.7 [206.4 and 197.6] [C_q, 1:4 C; *trans*- and *cis*-CO of W(CO)₅], 59.4 [64.7] (CH₂, C2), 37.0 [42.4] (SCH₂), 32.3 [34.7] (CH₂, C3), 22.9 [22.6] (CH₂, C4), 13.7 [13.7] (CH₃, C5), 11.6 [12.5] (SCH₂CH₃). IR (*n*-pentane): $\tilde{\nu}$ 2065.9 (60), 1957.6 (90), 1950.4 (100), 1935.5 (80) cm⁻¹ (C=O). MS (70 eV, EI): *m/z* (%) 454 (29) [M]⁺, 398 [M - 2CO]⁺, 397 (22), 370 (54) [M - 3CO]⁺, 342 [M - 4CO]⁺, 341 (94), 281 (100). Anal. Calcd (%) for C₁₂H₁₄O₅SW (454.2): C 31.72, H 3.11. Found: C 32.01, H 3.13.

Pentacarbonyl[1-(ethylthio)propylidene]tungsten (8b). Pentacarbonyl(1-ethoxypropylidene)tungsten (**7b**) (820 mg, 2.00 mmol),

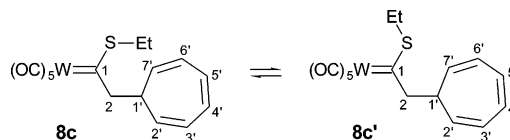
(22) (a) Aumann, R.; Runge, M. *Chem. Ber.* **1992**, *125*, 259–264. (b) Aumann, R.; Läge, M.; Krebs, B. *Chem. Ber.* **1994**, *127*, 731–738. (c) Aumann, R.; Fischer, E. O. *Angew. Chem.* **1967**, *79*, 900–901; *Angew. Chem., Int. Ed. Engl.* **1967**, *6*, 879–880.

(23) Axenrod, T.; Milne, G. W. A. *Tetrahedron* **1968**, *24*, 5775–5783.

sodium carbonate (254 mg, 2.40 mmol), and ethanethiol (248 mg, 4.00 mmol) were reacted for 1 h at -40 °C as described above to give compound **8b** (815 mg, 96%, *R_f* = 0.5 in *n*-pentane, red oil).

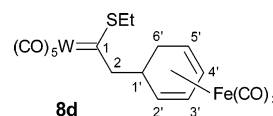
8b. ¹H NMR (400 MHz, CDCl₃, 25 °C): δ 3.81 (q, ³*J* = 7.7 Hz, 2H; 2-H₂), 3.01 (q, ³*J* = 7.6 Hz, 2H; SCH₂), 1.36 (t, ³*J* = 7.6 Hz, 3H; SCH₂CH₃), 1.30 (t, ³*J* = 7.7 Hz, 3H; 3-H₃). ¹³C NMR (CDCl₃, 25 °C): δ 339.7 (C_q, C1), 206.8 and 197.6 [C_q, 1:4 C; *trans*- and *cis*-CO of W(CO)₅], 52.4 (W=CCH₂), 36.8 (SCH₂), 14.2 (CH₂CH₃), 11.6 (SCH₂CH₃). IR (*n*-pentane): $\tilde{\nu}$ 2066.5 (50), 1957.9 (80), 1951.7 (100), 1938.8 (60) cm⁻¹ (C=O). MS (70 eV, EI): *m/z* (%) 426 (28) [M]⁺, 370 [M - 2CO]⁺, 369 (18), 342 (38) [M - 3CO]⁺, 314 [M - 4CO]⁺, 313 (100). Anal. Calcd (%) for C₁₀H₁₀O₅SW (426.1): C 28.17, H 2.37. Found: C 28.45, H 2.39.

Pentacarbonyl[2-(cyclohepta-2,4,6-trien-1-yl)-1-(ethylthio)ethylidene]tungsten (8c). Pentacarbonyl[2-(cyclohepta-2,4,6-trien-1-yl)-1-ethoxyethylidene]tungsten (**7c**) (972 mg, 2.00 mmol), sodium carbonate (254 mg, 2.40 mmol), and ethanethiol (248 mg, 4.00 mmol) were reacted for 6 h at -40 °C as described above to give a 3:1 mixture of **8c/8c'** and crystallized from *n*-pentane at -20 °C (950 mg, 95%, *R_f* = 0.8 in *n*-pentane/dichloromethane, 4:1, red crystals, mp 49 °C).



8c [8c']. ¹H NMR (400 MHz, CDCl₃, 25 °C): δ 6.65, 6.25, and 5.33 [6.67, 6.25, and 5.24] (m each, 2:2:2 H; from H-2' to H-7'), 3.94 [4.04] (q, ³*J* = 7.8 [7.4] Hz, 2H; 2-H₂), 2.99 [3.64] (q, ³*J* = 7.7 [7.5] Hz, 2H; SCH₂), 2.82 [2.56] (m, 1H; 1'-H of C₇H₇), 1.34 [1.56] (t, ³*J* = 7.7 [7.5] Hz, 3H; SCH₂CH₃). ¹³C NMR (CDCl₃, 25 °C): δ 334.9 (C_q, C1), 206.3 and 197.6 [C_q, 1:4 C; *trans*- and *cis*-CO of W(CO)₅], 131.1, 126.2, and 124.2 [131.1, 125.5, and 124.3] (CH, 2:2:2 C, from C-2' to C-7' of C₇H₇), 59.7 [67.0] (CH₂, C2), 41.7 [40.5] (CH, C1'), 38.3 [43.0] (SCH₂), 11.6 [12.4] (SCH₂CH₃). IR (*n*-pentane): $\tilde{\nu}$ 2066.1 (50), 1961.3 (60), 1949.9 (100), 1943.0 (90), 1935.6 (80) cm⁻¹ (C=O). MS (70 eV, EI): *m/z* (%) 502 [M]⁺, 446 [M - 2CO]⁺, 418 [M - 3CO]⁺, 390 [M - 4CO]⁺. Anal. Calcd (%) for C₁₆H₁₄O₅SW (502.0): C 38.25, H 2.81. Found: C 38.25, H 2.62.

Pentacarbonyl[1-(ethylthio)-2-{tricarbonyl(2,4-cyclohexadien-1-yl)iron}ethylidene]tungsten (8d). To pentacarbonyl[1-ethoxy-2-{tricarbonyl(2,4-cyclohexadien-1-yl)iron}ethylidene]tungsten (**7d**) (200 mg, 0.33 mmol) in dichloromethane/ether, 1:3 (2 mL), was added a mixture of ethanethiol (40 mg, 0.65 mmol) and triethylamine (66 mg, 0.65 mmol) in ether (0.5 mL) at -40 °C. Stirring was continued for 2–2.5 h at this temperature. After the consumption of the starting carbene complex, controlled by IR measurements, the reaction was quenched with phosphoric acid (2–3 drops). The afforded red solution was diluted with ether (30 mL) and then extracted with water (3 × 15 mL). Finally the organic phase was dried over magnesium sulfate, and the solvent was removed at reduced pressure to give **8d** (195 mg, 95%, *R_f* = 0.7 in *n*-pentane/dichloromethane, 4:1, red oil).



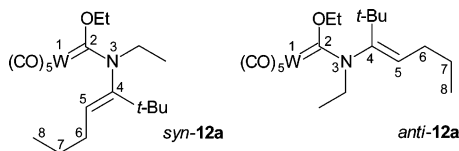
8d. ¹H NMR (400 MHz, C₆D₆, 25 °C): δ 4.76 (m, 1H; H-4'), 4.64 (m, 1H; 3'-H), 3.12 and 3.01 (m each, 1H each; 2-H₂), 2.87 (m, 1H; 1'-H), 2.71 (m, 1H; 2'-H), 2.57 (m, 1H; 5'-H), 2.09 (q, ³*J* = 7.7 Hz, 2H; SCH₂), 1.84 (ddd, 1H; δ' -endo-H), 0.89 (m, 1H; δ' -exo-H), 0.62 (t, ³*J* = 7.7 Hz, 3H; SCH₂CH₃). ¹³C NMR (C₆D₆, 25 °C): δ 333.7 (C_q, C1), 211.6 [C_q, CO of Fe(CO)₃], 206.2 and 198.1

[C_q, 1:4 C; *trans*- and *cis*-CO of W(CO)₅], 86.1 (CH, C-4'), 84.4 (CH, C-3'), 67.2 (CH₂, C2), 64.6 (CH, C2'), 59.2 (CH, C-5'), 41.3 (CH, C-1'), 38.0 (SCH₂), 29.7 (CH₂, C-6'), 11.2 (SCH₂CH₃). IR (*n*-pentane): $\tilde{\nu}$ 2066.6 (60), 2052.0 (70), 1992.6 (40), 1957.6 (95), 1952.2 (100), 1941.7 (90), 1933.5 (90) cm⁻¹ (C≡O). MS (70 eV, EI): *m/z* (%) 630 [M]⁺, 574 [M - 2CO]⁺, 490 [M - 5CO]⁺, 192 (100). HRMS (ESI⁻): *m/z* calcd for C₁₈H₁₃O₈SFeW 628.9200, found 628.9202.

Pentacarbonyl[1-(ethylthio)pentylidene]chromium (8e). Pentacarbonyl(1-ethoxypentylidene)chromium (**7e**) (612 mg, 2.00 mmol), sodium carbonate (254 mg, 2.40 mmol), and ethanethiol (248 mg, 4.00 mmol) were reacted for 1 h at -40 °C as described above to give compound **8e** (603 mg, 94%, *R_f* = 0.6 in *n*-pentane, red oil).

8e. ¹H NMR (400 MHz, C₆D₆, 25 °C): δ 3.46 (dd, ³*J* = 8.2 and 7.8 Hz, 2H; 2-H₂), 2.17 (q, ³*J* = 7.5 Hz, 2H; SCH₂), 1.36 (m, 2H; 3-H₂), 1.22 (m, 2H; 4-H₂), 0.80 (t, ³*J* = 7.5 Hz, 3H; SCH₂CH₃), 0.59 (t, ³*J* = 7.6 Hz, 3H; 5-H₃). ¹³C NMR (CDCl₃, 25 °C): δ 370.4 (C_q, Cr=C), 227.0 and 216.9 [C_q, 1:4 C; *trans*- and *cis*-CO of W(CO)₅], 58.0 (CH₂, C2), 36.2 (SCH₂), 32.3 (CH₂, C3), 23.0 (CH₂, C4), 13.7 (CH₃, C5), 11.2 (SCH₂CH₃). IR (*n*-pentane): $\tilde{\nu}$ 2058.0 (40), 1960.5 (100), 1939.4 (60) cm⁻¹ (C≡O). MS (70 eV, EI): *m/z* (%): 322 (13) [M]⁺, 294 (7) [M - CO]⁺, 266 (4) [M - 2CO]⁺, 238 (13), [M - 3CO]⁺, 210 (33) [M - 4CO]⁺, 182 (100) [M - 5CO]⁺. HRMS (ESI⁻): *m/z* calcd for C₁₂H₁₃O₅SCr 320.9883, found 320.9894.

(4E)-[2-Ethoxy-3-ethylamino-4-*tert*-butyl]-3-aza-1-pentacarbonyltungsta-1,4-diene (*syn*-12a** and *anti*-**12a**)**. To pentacarbonyl[1-ethoxypentylidene]tungsten (**7a**) (219 mg, 0.50 mmol) in dichloromethane (1 mL) in a 5 mL screw-top vessel was first added a mixture of *N*-ethyl-2,2-dimethylpropionimidoyl chloride (**9a**) (148 mg, 1.00 mmol) and *N,N*-dimethylamino pyridine (6 mg, 0.05 mmol) in dichloromethane (2 mL) at room temperature. Then to this reaction mixture was dropped triethylamine (51 mg, 0.50 mmol) in dichloromethane (0.5 mL) with stirring. The reaction was controlled by TLC and continued for 1 day at this temperature. After the consumption of compound **7a**, diethyl ether (10–15 mL) was added to the reaction mixture and the precipitate was removed by centrifugation. The solvent was evaporated at reduced pressure. Chromatography at 25 °C on silica gel (column 2 × 20 cm, *n*-pentane/dichloromethane, 95:5) afforded a pale yellow fraction with a 5:2 mixture of *syn*-**12a** and *anti*-**12a** (224 mg, 82%, *R_f* = 0.6 (*syn*-**12a**) and *R_f* = 0.7 (*anti*-**12a**) in *n*-pentane, pale yellow oil).



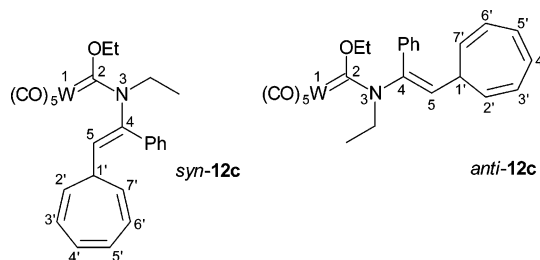
syn-12a. ¹H NMR (600 MHz, CDCl₃, 25 °C): δ 5.24 (dd, ³*J* = 10.4 and 4.4 Hz, 1H; 5-H), 4.57 (m, 2H; OCH₂), 4.19 and 2.85 (each m, each 1H; NCH₂), 2.42 and 2.28 (each m, each 1H; 6-H₂), 1.53 and 1.44 (each m, each 1H; 7-H₂), 1.44 (t, ³*J* = 7.0 Hz, 3H; OCH₂CH₃), 1.33 [s, 9H; C(CH₃)₃], 1.12 (t, ³*J* = 7.0 Hz, 3H; NCH₂CH₃), 0.98 (t, ³*J* = 7.3 Hz, 3H; 8-H₃). ¹³C NMR (CDCl₃, 25 °C): δ 229.9 (C_q, W=C), 200.5 and 199.0 [C_q, 1:4 C; *trans*- and *cis*-CO of W(CO)₅], 148.5 (C_q, C4), 135.8 (CH, C5), 73.2 (OCH₂), 47.1 (NCH₂), 34.9 [C_q, C(CH₃)₃], 30.5 [C(CH₃)₃], 30.3 (CH₂, C6), 22.8 (CH₂, C7), 15.4 (OCH₂CH₃), 13.9 (CH₃, C8), 11.7 (NCH₂CH₃). **anti-12a**. ¹H NMR (600 MHz, CDCl₃, 25 °C): δ 4.90 (t, ³*J* = 8.0 Hz, 1H; 5-H), 4.53 (m, 2H; OCH₂), 4.66 and 3.27 (each m, each 1H; NCH₂), 2.27 (m, 2H; 6-H₂), 1.46 (m, 2H; 7-H₂), 1.34 (t, ³*J* = 7.0 Hz, 3H; OCH₂CH₃), 1.26 (t, ³*J* = 7.1 Hz, 3H; NCH₂CH₃), 1.15 [s, 9H; C(CH₃)₃], 0.98 (t, ³*J* = 7.4 Hz, 3H; 8-H₃). ¹³C NMR (CDCl₃, 25 °C): δ 228.1 (C_q, W=C), 200.7 and 197.8 [C_q,

1:4 C; *trans*- and *cis*-CO of W(CO)₅], 145.9 (C_q, C4), 130.2 (CH, C5), 72.5 (OCH₂), 52.3 (NCH₂), 34.4 [C_q, C(CH₃)₃], 30.3 (CH₂, C6), 30.2 [C(CH₃)₃], 22.9 (CH₂, C7), 15.5 (OCH₂CH₃), 14.1 (NCH₂CH₃); 13.8 (CH₃, C8). IR (cyclohexane): $\tilde{\nu}$ 2064.3 (10), 1927.9 (100) cm⁻¹ (C≡O). MS (70 eV, EI): *m/z* (%): 549 (45) [M]⁺, 521 (27) [M - CO]⁺, 493 (34) [M - 2CO]⁺, 465 [M - 3CO]⁺, 463 (66), 437 [M - 4CO]⁺, 435 (75), 409 [M - 5CO]⁺, 407 (100). Anal. Calcd (%) for C₁₉H₂₇O₆NW (549.3): C 41.52, H 4.96, N 2.55. Found: C 41.83, H 4.97, N 2.89.

(4E)-[2-Ethoxy-3-ethylamino-4-*tert*-butyl]-3-aza-1-pentacarbonyltungstahexa-1,4-diene (*syn*-12b** and *anti*-**12b**)**. Pentacarbonyl[1-ethoxypropylidene]tungsten (**7b**) (205 mg, 0.50 mmol), *N*-ethyl-2,2-dimethylpropionimidoyl chloride (**9a**) (148 mg, 1.00 mmol), *N,N*-dimethylaminopyridine (6 mg, 0.05 mmol), and triethylamine (51 mg, 0.50 mmol) were reacted for 1 day as described above. Chromatography at 25 °C on silica gel (column 2 × 20 cm, *n*-pentane/dichloromethane, 95:5) afforded a pale yellow fraction with a 3:1 mixture of *syn*-**12b** and *anti*-**12b** (176 mg, 68%, *R_f* = 0.5 (*syn*-**12b**) and *R_f* = 0.6 (*anti*-**12b**) in *n*-pentane, pale yellow oil).

syn-12b. ¹H NMR (500 MHz, CDCl₃, 25 °C): δ 5.38 (q, ³*J* = 7.6 Hz, 1H; 5-H), 4.55 (m, 2H; OCH₂), 4.17 and 2.84 (each m, each 1H; NCH₂), 1.92 (d, ³*J* = 7.6 Hz, 3H; 6-H₃), 1.44 (t, ³*J* = 6.9 Hz, 3H; OCH₂CH₃), 1.32 [s, 9H; C(CH₃)₃], 1.11 (t, ³*J* = 6.9 Hz, 3H; NCH₂CH₃). ¹³C NMR (CDCl₃, 25 °C): δ 230.0 (C_q, W=C), 200.5 and 199.0 [C_q, 1:4 C; *trans*- and *cis*-CO of W(CO)₅], 149.5 (C_q, C4), 129.8 (CH, C5), 73.2 (OCH₂), 47.2 (NCH₂), 34.8 [C_q, C(CH₃)₃], 30.2 [C(CH₃)₃], 15.4 (OCH₂CH₃), 14.3 (CH₃, C6), 11.8 (NCH₂CH₃). **anti-12b**. ¹H NMR (500 MHz, CDCl₃, 25 °C): δ 5.02 (q, ³*J* = 7.6 Hz, 1H; 5-H), 4.52 (q, 2H; OCH₂), 4.65 and 3.28 (each m, each 1H; NCH₂), 1.86 (d, ³*J* = 7.6 Hz, 3H; 6-H₃), 1.34 (t, ³*J* = 7.1 Hz, 3H; OCH₂CH₃), 1.25 (t, ³*J* = 7.2 Hz, 3H; NCH₂CH₃), 1.16 [s, 9H; C(CH₃)₃]. ¹³C NMR (CDCl₃, 25 °C): δ 228.2 (C_q, W=C), 200.7 and 197.8 [C_q, 1:4 C; *trans*- and *cis*-CO of W(CO)₅], 146.8 (C_q, C4), 123.9 (CH, C5), 72.5 (OCH₂), 52.3 (NCH₂), 34.3 [C_q, C(CH₃)₃], 29.7 [C(CH₃)₃], 15.5 (OCH₂CH₃), 14.1 (NCH₂CH₃), 13.9 (CH₃, C6). IR (cyclohexane): $\tilde{\nu}$ 2064.2 (10), 1927.5 (100) cm⁻¹ (C≡O). MS (70 eV, EI): *m/z* (%) 521 (37) [M]⁺, 493 (22) [M - CO]⁺, 465 (35) [M - 2CO]⁺, 437 (14) [M - 3CO]⁺, 406 (40), 381 (100) [M - 5CO]⁺. HRMS (ESI⁺): *m/z* calcd for C₁₇H₂₃NO₆-WNa 544.0930, found 544.0917 [M + Na]⁺.

(4E)-[(5-Cyclohepta-2,4,6-trien-1-yl)-2-ethoxy-3-ethylamino-4-phenyl]-3-aza-1-pentacarbonyltungstapenta-1,4-diene (*syn*-12c** and *anti*-**12c**)**. Pentacarbonyl[2-(cyclohepta-2,4,6-trien-1-yl)-1-ethoxythylidene]tungsten (**7c**) (243 mg, 0.50 mmol), *N*-ethylbenzimidoyl chloride (**9b**) (168 mg, 1.00 mmol), *N,N*-dimethylaminopyridine (6 mg, 0.05 mmol), and triethylamine (51 mg, 0.50 mmol) were reacted for 1 day as described above. Chromatography at 25 °C on silica gel (column 2 × 20 cm, *n*-pentane/dichloromethane, 95:5) afforded a pale yellow fraction with a 10:9 mixture of *syn*-**12c** and *anti*-**12c** (215 mg, 70%, *R_f* = 0.8 (for both isomers) in *n*-pentane/dichloromethane, 4:1, pale yellow oil).



syn-12c. ¹H NMR (500 MHz, CDCl₃, 25 °C): δ 7.33–7.29 and 7.11 (each m, 8:2 H, *o*-, *m*-, *p*-H of both *syn*- and *anti*-isomers), 6.68 (m, 2H; 4'-H and 5'-H), 6.36 and 6.26 (each m, each 1H; 3'-H and 6'-H), 6.18 (d, ³*J* = 10.4 Hz, 1H; 5-H), 5.41 and 5.27 (four-line pattern, each 1H; 2'-H and 7'-H), 4.67 and 4.61 (q, AB

system, $^3J = 7.0$ Hz, 2H; OCH₂), 4.02 and 2.84 (each q, $^3J = 7.2$ Hz, 2H; NCH₂), 2.68 (m, 1H; 1'-H), 1.51 (t, $^3J = 7.0$ Hz, 3H; OCH₂CH₃), 1.13 (t, $^3J = 7.2$ Hz, 3H; NCH₂CH₃). ¹³C NMR (CDCl₃, 25 °C): δ 232.1 (C_q, W=C), 200.6 and 199.0 [C_q, 1:4 C; *trans*- and *cis*-CO of W(CO)₅], 143.6 (C_q, C4), 134.4 (CH, C5), 133.7 (C_q, *i*-C Ph), 131.6 and 130.3 (each CH, C4' and C5'), 129.1, 129.0, 128.6, 128.5, 128.4, 128.0 (each CH, *o*-, *m*-, and *p*-C Ph of both *syn*- and *anti*-isomers), 125.1 (2 signals, each CH, C3' and C6'), 121.2 and 120.0 (each CH, C2' and C7'), 74.1 (OCH₂), 45.8 (NCH₂), 38.6 (CH, C1'); 15.4 (OCH₂CH₃), 13.1 (NCH₂CH₃). **anti-12c**. ¹H NMR (500 MHz, CDCl₃, 25 °C): δ 6.66 (m, 2H; 4'-H and 5'-H), 6.24 (m, 2H; 3'-H and 6'-H), 5.79 (d, $^3J = 10.4$ Hz, 1H; 5-H), 5.23 (four-line pattern, 2H; 2'-H and 7'-H), 4.58 (q, $^3J = 7.0$ Hz, 2H; OCH₂), 4.02 (s, br, 2H; NCH₂), 2.63 (m, 1H; 1'-H), 1.31 (t, $^3J = 7.2$ Hz, 3H; NCH₂CH₃) 1.26 (t, $^3J = 7.0$ Hz, 3H; OCH₂-CH₃). ¹³C NMR (CDCl₃, 25 °C): δ 231.0 (C_q, W=C), 200.9 and 197.7 [C_q, 1:4 C; *trans*- and *cis*-CO of W(CO)₅], 139.2 (C_q, C4), 134.0 (C_q, *i*-C Ph), 131.7 (CH, C5), 131.2 (CH, C4' and C5'), 124.9 (CH, C3' and C6'), 123.5 (CH, C2' and C7'), 73.1 (OCH₂), 51.3 (NCH₂), 38.6 (CH, C1'), 15.2 (OCH₂CH₃), 14.2 (NCH₂CH₃). IR (cyclohexane): $\tilde{\nu}$ 2064.8 (10), 1929.4 (100), 1916.5 (30) cm⁻¹ (C≡O). MS (70 eV, EI): m/z (%) 617 (2) [M]⁺, 589 (3) [M - CO]⁺, 533 (5) [M - 3CO]⁺, 483 (12). HRMS (ESI⁺): m/z calcd for C₂₅H₂₃NO₆WNa 640.0931, found 640.0940 [M + Na]⁺.

(4E)-[2-Ethoxy-3-ethylamino-4-phenyl]-3-aza-1-pentacarbonyl-tungsta-octa-1,4-diene (syn-12d and anti-12d). Pentacarbonyl-[1-ethoxypropylidene]tungsten (**7a**) (219 mg, 0.50 mmol), *N*-ethylbenzimidoyl chloride (**9b**) (168 mg, 1.00 mmol), *N,N*-dimethylaminopyridine (6 mg, 0.05 mmol), and triethylamine (51 mg, 0.50 mmol) were reacted for 1 day as described above. Chromatography at 25 °C on silica gel (column 2 × 20 cm, *n*-pentane/dichloromethane, 95:5) afforded a pale yellow fraction with a 2:1 mixture of *syn*-**12d** and *anti*-**12d** (202 mg, 71%, *R_f* = 0.5 (*syn*-**12d**) and *R_f* = 0.6 (*anti*-**12d**) in *n*-pentane, pale yellow oil).

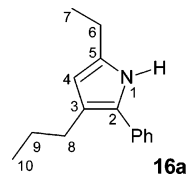
syn-12d. ¹H NMR (400 MHz, CDCl₃, 25 °C): δ 7.39–7.32 and 7.18 (each m, 8:2 H, *o*-, *m*-, *p*-H Ph of both *syn*- and *anti*-isomers), 5.86 (dd, $^3J = 7.1$ and 8.0 Hz, 1H; 5-H), 4.65 and 4.63 (q, AB system, $^3J = 7.0$ Hz, 2H; OCH₂), 4.0 and 2.82 (each m, each 1H; NCH₂), 2.50 and 2.38 (each m, each 1H; 6-H₂), 1.65 (m, 2H; 7-H₂), 1.48 (t, $^3J = 7.0$ Hz, 3H; OCH₂CH₃), 1.10 (t, $^3J = 7.1$ Hz, 3H; NCH₂CH₃), 1.04 (t, $^3J = 7.2$ Hz, 3H, 8-H₃). ¹³C NMR (CDCl₃, 25 °C): δ 232.0 (C_q, W=C), 200.8 and 198.8 [C_q, 1:4 C; *trans*- and *cis*-CO of W(CO)₅], 142.3 (C_q, C4), 134.8 (CH, C5), 134.3 (C_q, *i*-C Ph), 129.1, 128.7, 128.4, 128.3, 128.1 (each CH, *o*-, *m*-, and *p*-C Ph of both *syn*- and *anti*-isomers), 73.7 (OCH₂), 45.7 (NCH₂), 31.1 (CH₂, C6), 22.5 (CH₂, C7), 15.4 (OCH₂CH₃), 14.1 (CH₃, C8), 13.1 (NCH₂CH₃). **anti-12d**. ¹H NMR (400 MHz, CDCl₃, 25 °C): δ 5.43 (t, $^3J = 7.7$ Hz, 1H; 5-H), 4.56 (q, $^3J = 7.0$ Hz, 2H; OCH₂), 4.0 (q, 2H; NCH₂), 2.29 (q, $^3J = 7.5$ Hz, 1H; 6-H₂), 1.48 (m, 2H; 7-H₂), 1.25 (t, $^3J = 7.1$ Hz, 3H; NCH₂CH₃), 1.23 (t, $^3J = 7.0$ Hz, 3H; OCH₂CH₃), 0.93 (t, $^3J = 7.4$ Hz, 3H, 8-H₃). ¹³C NMR (CDCl₃, 25 °C): δ 230.4 (C_q, W=C), 200.6 and 197.8 [C_q, 1:4 C; *trans*- and *cis*-CO of W(CO)₅], 137.8 (C_q, C4), 134.8 (C_q, *i*-C Ph), 131.4 (CH, C5), 72.9 (OCH₂), 51.4 (NCH₂), 30.4 (CH₂, C6), 22.9 (CH₂, C7), 15.2 (OCH₂CH₃), 14.1 (NCH₂CH₃), 13.8 (CH₃, C8). IR (cyclohexane): $\tilde{\nu}$ 2062.6 (10), 1928.4 (100), 1916.4 (30) cm⁻¹ (C≡O). MS (70 eV, EI): m/z (%) 569 (8) [M]⁺, 541 (18) [M - CO]⁺, 485 (100) [M - 3CO]⁺. HRMS (ESI⁺): m/z calcd for C₂₁H₂₃NO₆WNa 592.0930, found 592.0934 [M + Na]⁺.

(4E)-[2-Ethoxy-3-isopropylamino-4-tert-butyl]-3-aza-1-pentacarbonyl-tungsta-hexa-1,4-diene (anti-12e). Pentacarbonyl-[1-ethoxypropylidene]tungsten (**7b**) (205 mg, 0.50 mmol), *N*-isopropyl-2,2-dimethylpropionimidoyl chloride (**9c**) (162 mg, 1.00 mmol), *N,N*-dimethylaminopyridine (6 mg, 0.05 mmol), and triethylamine (51 mg, 0.50 mmol) were reacted for 1 day as described above. Chromatography at 25 °C on silica gel (column 2 × 20 cm,

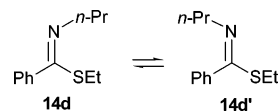
n-pentane/dichloromethane, 95:5) afforded a pale yellow fraction of *anti*-**12e** (162 mg, 61%, *R_f* = 0.5 in *n*-pentane, pale yellow oil).

anti-12e. ¹H NMR (400 MHz, CDCl₃, 25 °C): δ 5.31 (sep, $^3J = 6.7$ Hz, 1H; NCH), 5.15 (q, $^3J = 7.6$ Hz 1H; 5-H), 4.67 and 4.52 (q, AB system, $^3J = 7.1$ Hz, 2H; OCH₂), 1.87 (d, $^3J = 7.6$ Hz, 3H; 6-H₃), 1.36 (t, $^3J = 7.1$ Hz, 3H; OCH₂CH₃), 1.29 and 1.28 [each d, $^3J = 6.7$ Hz, each 3H; NCH(CH₃)₂], 1.18 [s, 9H; C(CH₃)₃]. ¹³C NMR (CDCl₃, 25 °C): δ 230.6 (C_q, W=C), 201.0 and 197.8 [C_q, 1:4 C; *trans*- and *cis*-CO of W(CO)₅], 146.6 (C_q, C4), 123.3 (CH, C5), 72.8 (OCH₂), 59.0 (NCH), 34.5 [C_q, C(CH₃)₃], 29.8 [C(CH₃)₃], 25.2 and 20.2 [NCH(CH₃)₂], 15.7 (OCH₂CH₃), 14.3 (CH₃, C6). IR (cyclohexane): $\tilde{\nu}$ 2064.0 (10), 1927.8 (100) cm⁻¹ (C≡O). MS (70 eV, EI): m/z (%) 535 (40) [M]⁺, 507 (34) [M - CO]⁺, 479 (28) [M - 2CO]⁺, 451 (15) [M - 3CO]⁺, 420 (36), 395 [M - 5CO]⁺, 393 (100). HRMS (ESI⁺): m/z calcd for C₁₈H₂₅-NO₆WNa 558.1086, found 558.1076 [M + Na]⁺.

5-Ethyl-2-phenyl-3-propyl-1H-pyrrole (16a) and N-Propylthiobenzimidic acid Ethyl Ester (14d and 14d'). To a mixture of pentacarbonyl[1-(ethylthio)propylidene]tungsten (**8a**) (454 mg, 1.00 mmol) and *N*-propylbenzimidoyl chloride (**9d**) (363 mg, 2.00 mmol) in diethyl ether (3 mL) in a 5 mL flask was added triethylamine (101 mg, 1.00 mmol) in diethyl ether (0.5 mL) with stirring at -40 °C. The stirring was continued for 10–15 min at this temperature. After the consumption of **8a** (controlled by TLC), the reaction mixture was centrifuged, the precipitate was removed, and the solvent was evaporated at reduced pressure. The ¹H NMR spectrum indicated the formation of **16a**, **14d**, and **14d'** in a ratio of 3:2:1, respectively. Chromatography at 25 °C on silica gel (column 2 × 20 cm, *n*-pentane/dichloromethane, 4:1) afforded compound **16a** (166 mg, 78%, *R_f* = 0.4 in *n*-pentane/dichloromethane, 4:1, yellowish oil). Isomers **14d** and **14d'** were not isolated and characterized from the ¹H NMR spectrum of the reaction mixture.



16a. ¹H NMR (400 MHz, CDCl₃, 25 °C): δ 7.74 (s, br, 1H; NH), 7.36–7.35 (m, 4H; *o*-, and *m*-H Ph), 7.22–7.17 (m, 1H; *p*-H Ph), 5.89 (d, br, 1H; $^4J = 3.0$ Hz, 4-H), 2.63 (dq, $^4J = 0.8$ and $^3J = 7.6$ Hz, 2H; 6-H₂), 2.57 (dd, $^3J = 7.7$ and 7.9 Hz, 2H; 8-H₂), 1.64 (m, 2H; 9-H₂), 1.26 (t, 3H; 7-H₃), 0.96 (t, $^3J = 7.4$ Hz, 3H; 10-H₃). ¹³C NMR (CDCl₃, 25 °C): 134.1 and 134.0 (each C_q, *i*-C Ph and/or C5), 128.6, 126.4 and 125.6 (each CH, *o*-, *m*-, and *p*-C Ph), 126.4 (C_q, C2), 121.7 (C_q, C3), 106.8 (CH, C4), 28.8 (CH₂, C8), 24.3 (CH₂, C9), 20.9 (CH₂, C6), 14.3 (CH₃, C10), 13.4 (CH₃, C7). IR (film): $\tilde{\nu}$ 3468.7, br, 3426.6, 3392.1 br cm⁻¹ (N-H). MS (70 eV, EI): m/z (%) 213 (38) [M]⁺, 198 (25), 184 (100), 168 (52), 155 (22), 77 (12). Anal. Calcd (%) for C₁₅H₁₉N (213.3): C 84.46, H 8.98, N 6.57. Found: C 84.42, H 8.87, N 6.50.



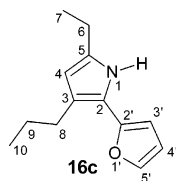
14d [14d']. ¹H NMR (300 MHz, CDCl₃, 25 °C): δ 7.53, 7.37, and 7.23 (each m, 10H; *o*-, *m*-, and *p*-H Ph of both isomers), 3.60 [3.27] (dd, $^3J = 6.9$ [6.9] and 7.2 [7.0] Hz, 2H; NCH₂), 2.58 [3.03] (q, $^3J = 7.4$ [7.4] Hz, 2H; SCH₂), 1.79 [1.59] (m, 2H; NCH₂CH₂), 1.08 [1.32] (t, $^3J = 7.4$ [7.4] Hz, 3H; SCH₂CH₃), 1.01 [0.87] (t, $^3J = 7.4$ [7.4] Hz, 3H; NCH₂CH₂CH₃).

2,5-Diphenyl-3-propyl-1H-pyrrole (16b) and N-Benzylthiobenzimidic Acid Ethyl Ester (14e and 14e'). Pentacarbonyl[1-(ethylthio)pentylidene]tungsten (**8a**) (454 mg, 1.00 mmol), *N*-benzylbenzimidoyl chloride (**9e**) (459 mg, 2.00 mmol), and triethylamine (101 mg, 1.00 mmol) were reacted as described above to give compounds **16b** (182 mg, 70%, $R_f = 0.4$ in *n*-pentane/dichloromethane, 4:1, yellowish oil), **14e**, and **14e'**.

16b. ^1H NMR (400 MHz, CDCl_3 , 25 °C): δ 8.18 (s, br, 1H; NH), 7.45–7.11 (m, 10 H; *o*-, *m*-, and *p*-H Ph), 6.46 (d, br, $^4J = 3.2$ Hz, 1H; 4-H), 2.60 (dd, $^3J = 7.6$ and 7.9 Hz, 2H; 6-H₂), 1.67 (m, 2H; 7-H₂), 0.97 (t, $^3J = 7.4$ Hz, 3H; 8-H₃). ^{13}C NMR (CDCl_3 , 25 °C): 133.5 and 132.5 (each C_q, *i*-C Ph), 131.5 (C_q, C5), 129.3 (C_q, C2), 128.8, 128.7, 126.7, 126.2, 126.0, and 123.5 (each CH, *o*-, *m*-, and *p*-C Ph), 123.5 (C_q, C3), 108.3 (CH, C4), 28.7 (CH₂, C6), 24.2 (CH₂, C7), 14.2 (CH₃, C8). IR (film): $\tilde{\nu}$ 3436.4, 3380.0, br cm^{-1} (N–H). MS (70 eV, EI): m/z (%): 261 (100) [M]⁺, 232 (96), 194 (15), 91 (63). Anal. Calcd (%) for C₁₉H₁₉N (261.4): C 87.31, H 7.33, N 5.36. Found: C 87.40, H 7.28, N 5.55.

14e [14e']. ^1H NMR (400 MHz, CDCl_3 , 25 °C): δ 7.58, 7.42–7.18 (each m, 20H; *o*-, *m*-, and *p*-H Ph of both isomers), 4.87 [4.54] (s, 2H; NCH₂), 2.62 [3.09] (q, $^3J = 7.4$ [7.5] Hz, 2H; SCH₂), 1.08 [1.34] (t, $^3J = 7.4$ [7.5] Hz, 3H; SCH₂CH₃).

5-Ethyl-2-(2-furyl)-3-propyl-1H-pyrrole (16c) and N-Propylfuran-2-carboximidothioic Acid Ethyl Ester (14f and 14f'). Pentacarbonyl[1-(ethylthio)pentylidene]tungsten (**8a**) (454 mg, 1.00 mmol), *N*-propylfuran-2-carboximidoyl chloride (**9f**) (343 mg, 2.00 mmol), and triethylamine (101 mg, 1.00 mmol) were reacted as described above to give compounds **16c** (104 mg, 51%, $R_f = 0.5$ in *n*-pentane/dichloromethane, 4:1, yellowish oil), **14f**, and **14f'**.



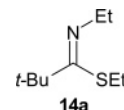
16c. ^1H NMR (600 MHz, CDCl_3 , 25 °C): δ 8.11 (s, br, 1H; NH), 7.32 (dd, $^4J = 0.6$ Hz, $^3J = 1.8$ Hz, 1H; 5'-H), 6.43 (dd, $^3J = 1.8$ Hz, $^3J = 3.3$ Hz, 1H; 4'-H), 6.20 (dd, $^4J = 0.6$ Hz, $^3J = 3.3$ Hz, 1H; 3'-H), 5.83 (d, br, $^4J = 3.1$ Hz, 1H; 4-H), 2.63 (dq, $^4J = 0.5$ and $^3J = 7.6$ Hz, 2H; 6-H₂), 2.55 (dd, $^3J = 7.6$ and 7.8 Hz, 2H; 8-H₂), 1.63 (m, 2H; 9-H₂), 1.26 (t, 3H; 7-H₃), 0.99 (t, $^3J = 7.4$ Hz, 3H; 10-H₃). ^{13}C NMR (CDCl_3 , 25 °C): 148.5 (C_q, C2'), 139.3 (CH, C5'), 134.0 (C_q, C5), 122.0 (C_q, C3), 118.4 (C_q, C2), 111.4 (CH, C4'), 106.7 (CH, C4), 101.9 (CH, C3'), 28.9 (CH₂, C8), 23.4 (CH₂, C9), 20.9 (CH₂, C6), 14.2 (CH₃, C10), 13.5 (CH₃, C7). IR (film): $\tilde{\nu}$ 3473.8, 3424.9 (br cm^{-1} (N–H)). MS (70 eV, EI): m/z (%) 203 (59) [M]⁺, 188 (41), 174 (100), 146 (21), 130 (37), 117 (31), 77 (11), 55 (18). Anal. Calcd (%) for C₁₃H₁₇NO (203.3): C 76.81, H 8.43, N 6.89. Found: C 76.85, H 8.50, N 6.92.

14f [14f']. ^1H NMR (400 MHz, CDCl_3 , 25 °C): δ 7.50 [7.49] (dd, $^3J = 1.7$ [1.8] and $^4J = 0.8$ [0.8] Hz, 1H; 5'-H), 6.87 [6.75] (d, br, $^3J = 3.3$ [3.3] Hz, 1H; 3'-H), 6.45 [6.46] (dd, $^3J = 3.3$ [3.3] and $^3J = 1.7$ [1.8] Hz, 1H; 4'-H), 3.69 [3.62] (dd, $^3J = 6.8$ and 7.2 [6.4 and 7.2] Hz, 2H; NCH₂), 2.88 [3.0] (q, $^3J = 7.4$ [7.5] Hz, 2H; SCH₂), 1.77 [1.73] (m, 2H; NCH₂CH₂), 1.21 [1.30] (t, $^3J = 7.4$ [7.5] Hz, 3H; SCH₂CH₃), 0.99 [0.98] (t, $^3J = 7.4$ [7.4] Hz, 3H; NCH₂CH₂CH₃).

2-tert-Butyl-5-methyl-3-propyl-1H-pyrrole (16d) and N-Ethyl-2,2-dimethylthiopropionimidic Acid Ethyl Ester (14a) (from 8a). Pentacarbonyl[1-(ethylthio)pentylidene]tungsten (**8a**) (454 mg, 1.00 mmol), *N*-ethyl-2,2-dimethylpropionimidoyl chloride (**9a**) (295 mg, 2.00 mmol), and triethylamine (101 mg, 1.00 mmol) were reacted as described above to give compounds **16d** (143 mg, 80%, $R_f = 0.5$ in *n*-pentane/dichloromethane, 4:1, yellowish oil) and **14a**.

16d. ^1H NMR (400 MHz, CDCl_3 , 25 °C): δ 7.43 (s, br, 1H; NH), 5.69 (d, br, $^4J = 2.8$ Hz, 1H; 4-H), 2.48 (dd, $^3J = 7.8$ and 8.3

Hz, 2H; 7-H₂), 2.19 (d, br, $^4J = 0.5$ Hz, 3H; 6-H₃), 1.58 (m, 2H; 8-H₂), 1.33 [s, 9H; C(CH₃)₃], 0.97 (t, $^3J = 7.4$ Hz, 3H; 9-H₃). ^{13}C NMR (CDCl_3 , 25 °C): 132.8 (C_q, C2), 123.1 (C_q, C5), 118.6 (C_q, C3), 108.2 (CH, C4), 32.1 [C_q, C(CH₃)₃], 30.6 [C(CH₃)₃], 29.6 (CH₂, C7), 24.9 (CH₂, C8), 14.4 (CH₃, C9), 12.8 (CH₃, C6). IR (film): $\tilde{\nu}$ 3490.8, 3418.5, br cm^{-1} (N–H). MS (70 eV, EI): m/z (%): 179 (22) [M]⁺, 164 (100), 135 (11), 85 (10). Anal. Calcd (%) for C₁₂H₂₁N (179.3): C 80.38, H 11.81, N 7.82. Found: C 80.26, H 11.70, N 7.64.



14a. ^1H NMR (400 MHz, CDCl_3 , 25 °C): δ 3.59 (q, $^3J = 7.2$ Hz, 2H; NCH₂), 2.71 (q, $^3J = 7.6$ Hz, 2H; SCH₂), 1.23 (t, $^3J = 7.2$ Hz, 3H; NCH₂CH₃), 1.22 (t, $^3J = 7.6$ Hz, 3H; SCH₂CH₃), 1.19 [s, 9H; C(CH₃)₃].

5-Methyl-2-phenyl-3-propyl-1H-pyrrole (16e) and N-Ethylthiobenzimidic Acid Ethyl Ester (14b and 14b') (from 8a). Pentacarbonyl[1-(ethylthio)pentylidene]tungsten (**8a**) (454 mg, 1.00 mmol), *N*-ethylbenzimidoyl chloride (**9b**) (335 mg, 2.00 mmol), and triethylamine (101 mg, 1.00 mmol) were reacted as described above to give compounds **16e** (141 mg, 71%, $R_f = 0.4$ in *n*-pentane/dichloromethane, 4:1, yellowish oil), **14b**, and **14b'**.

16e. ^1H NMR (500 MHz, CDCl_3 , 25 °C): δ 7.76 (s, br, 1H; NH), 7.37–7.36 (m, 4H; *o*-, and *m*-H Ph), 7.23–7.19 (m, 1H; *p*-H Ph), 5.87 (d, br, $^4J = 2.5$ Hz, 1H; 4-H), 2.56 (dd, $^3J = 7.8$ and 7.9 Hz, 2H; 7-H₂), 2.30 (s, 3H; 6-H₃), 1.63 (m, 2H, 8-H₂), 0.96 (t, $^3J = 7.4$ Hz, 3H; 9-H₃). ^{13}C NMR (CDCl_3 , 25 °C): 134.0 (C_q, *i*-C Ph), 128.6, 126.4, and 125.6 (each CH, *o*-, *m*-, and *p*-C Ph), 127.5 (C_q, C5), 126.6 (C_q, C2), 121.9 (C_q, C3), 108.6 (CH, C4), 28.7 (CH₂, C7), 24.4 (CH₂, C8), 14.3 (CH₃, C9), 13.1 (CH₃, C6). IR (film): $\tilde{\nu}$ 3423.8, 3374.9, br cm^{-1} (N–H). MS (70 eV, EI): m/z (%) 199 (33) [M], 170 (100), 128 (14), 77 (13). Anal. Calcd (%) for C₁₄H₁₇N (199.3): C 84.37, H 8.60, N 7.03. Found: C 84.30, H 8.55, N 6.97.

14b [14b']. ^1H NMR (400 MHz, CDCl_3 , 25 °C): δ 7.52, 7.36, and 7.23 (each m, 10H; *o*-, *m*-, and *p*-H Ph of both isomers), 3.66 [3.33] (q, $^3J = 7.2$ [7.2] Hz, 2H; NCH₂), 2.56 [3.0] (q, $^3J = 7.5$ [7.4] Hz, 2H; SCH₂), 1.34 [1.14] (t, $^3J = 7.2$ [7.2] Hz, 3H; NCH₂CH₃), 1.06 [1.31] (t, $^3J = 7.5$ [7.4] Hz, 3H; SCH₂CH₃).

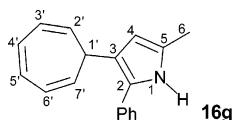
2-tert-Butyl-3,5-dimethyl-1H-pyrrole (16f) and N-Ethyl-2,2-dimethylthiopropionimidic Acid Ethyl Ester (14a). Pentacarbonyl[1-(ethylthio)propylidene]tungsten (**8b**) (426 mg, 1.00 mmol), *N*-ethyl-2,2-dimethylpropionimidoyl chloride (**9a**) (295 mg, 2.00 mmol), and triethylamine (101 mg, 1.00 mmol) were reacted as described above to give compounds **16f** (113 mg, 75%, $R_f = 0.5$ in *n*-pentane/dichloromethane, 4:1, yellowish oil) and **14a**.

16f. ^1H NMR (400 MHz, CDCl_3 , 25 °C): δ 7.47 (s, br, 1H; NH), 5.63 (d, br, $^4J = 3.1$ Hz, 1H; 4-H), 2.18 (d, br, $^4J = 0.7$ Hz, 3H; 6-H₃), 2.13 (s, 3H; 7-H₃), 1.32 [s, 9H; C(CH₃)₃]. ^{13}C NMR (CDCl_3 , 25 °C): 133.2 (C_q, C2), 122.9 (C_q, C5), 112.6 (C_q, C3), 109.9 (CH, C4), 32.1 [C_q, C(CH₃)₃], 30.1 [C(CH₃)₃], 13.2 and 12.7 (each CH₃, C-6 and C-7). IR (film): $\tilde{\nu}$ 3490.2, 3416.4 (br cm^{-1} (N–H)). MS (70 eV, EI): m/z (%): 151 (35) [M]⁺, 136 (100), 70 (18), 61 (23). Anal. Calcd (%) for C₁₀H₁₇N (151.3): C 79.41, H 11.33, N 9.26. Found: C 79.43, H 11.30, N 9.24.

14a. See above at the synthesis of **16d** for spectroscopic data.

3-Cyclohepta-2,4,6-trien-1-yl-5-methyl-2-phenyl-1H-pyrrole (16g) and N-Ethylthiobenzimidic Acid Ethyl Ester (14b and 14b'). Pentacarbonyl[2-(cyclohepta-2,4,6-trien-1-yl)-1-(ethylthio)ethylidene]tungsten (**8c**) (502 mg, 1.00 mmol), *N*-ethylbenzimidoyl chloride (**9b**) (335 mg, 2.00 mmol), and triethylamine (101 mg, 1.00 mmol) were reacted as described above to give compounds

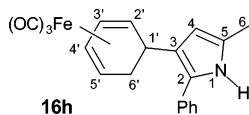
16g (175 mg, 71%, $R_f = 0.3$ in *n*-pentane/dichloromethane, 4:1, colorless crystals from *n*-pentane/dichloromethane, 4:1, at $-20\text{ }^\circ\text{C}$, mp $101\text{ }^\circ\text{C}$), **14b**, and **14b'**.



16g. ^1H NMR (500 MHz, CDCl_3 , $25\text{ }^\circ\text{C}$): δ 7.82 (s, br, 1H; NH), 7.30–7.14 (m, 5H; *o*-, *m*-, and *p*-H Ph), 6.68, 6.20, and 5.45 (each m, 2:2:2 H; from 2'-H to 7'-H), 6.12 (d, br, $^4J = 2.3$ Hz, 1H; 4-H), 2.78 (t, br, $^3J = 5.4$ Hz, 1H; 1'-H), 2.34 (s, 3H; 6- H_3). ^{13}C NMR (CDCl_3 , $25\text{ }^\circ\text{C}$): 133.3 (C_q , *i*-C Ph), 130.8, 127.6, 123.8 (each CH, 2:2:2 C; from C2' to C7'), 128.6, 126.6, and 126.0 (each CH, *o*-, *m*-, and *p*-C Ph), 128.2 (C_q , C5), 127.6 (C_q , C2), 123.4 (C_q , C3), 106.6 (CH, C4), 37.3 (CH, C1'), 13.2 (CH_3 , C6). IR (film): $\tilde{\nu}$ 3421.9, 3371.0, br cm^{-1} (N-H). MS (70 eV, EI): m/z (%) 247 (100) $[\text{M}]^+$, 170 (46), 127 (10), 57 (41). Anal. Calcd (%) for $\text{C}_{18}\text{H}_{17}\text{N}$ (247.3): C 87.41, H 6.93, N 5.66. Found: C 87.19, H 6.79, N 5.91.

14b and **14b'**. See above at the synthesis of **16e** for spectroscopic data.

3-[Tricarbonyl(2,4-cyclohexadien-1-yl)iron]-5-methyl-2-phenyl-1H-pyrrole (16h) and N-Ethylthiobenzimidic Acid Ethyl Ester (14b and 14b'). Pentacarbonyl[1-(ethylthio)-2-{tricarbonyl(2,4-cyclohexadien-1-yl)iron}ethylidene]tungsten (**8d**) (315 mg, 0.50 mmol), *N*-ethylbenzimidoyl chloride (**9b**) (168 mg, 1.00 mmol), and triethylamine (51 mg, 0.50 mmol) were reacted as described above to give compounds **16h** (120 mg, 64%, $R_f = 0.3$ in *n*-pentane/dichloromethane, 4:1, yellow crystals from *n*-pentane/dichloromethane, 4:1, at $-20\text{ }^\circ\text{C}$, 4/1, $146\text{--}147\text{ }^\circ\text{C}$), **14b**, and **14b'**.



16h. ^1H NMR (400 MHz, C_6D_6 , $25\text{ }^\circ\text{C}$): δ 6.77 (s, br, 1H; NH), 7.21–7.15 and 7.06 (each m, 4:1 H; *o*-, *m*-, and *p*-H Ph), 5.73 (d, br, $^4J = 2.1$ Hz, 1H; 4-H), 4.91 (m, 1H; 2'-H), 4.84 (m, 1H; 3'-H), 3.61 (dt, $^3J = 11.1$ and 3.6 Hz, 1H; 5'-H), 2.98 (m, 1H; 4'-H), 2.71 (m, 1H; 1'-H), 2.13 (m, 1H; 6'- endo-H), 1.89 (d, br, $^4J = 0.4$ Hz, 3H; 6- H_3), 1.56 (m, 1H; 6'- exo-H). ^{13}C NMR (CDCl_3 , $25\text{ }^\circ\text{C}$): 133.3 (C_q , *i*-C Ph), 128.8, 126.9, and 126.3 (each CH, *o*-, *m*-, and *p*-C Ph), 128.0, 127.1, and 126.4 (each C_q , C5, C2, and C3), 105.9 (CH, C4), 86.0 (CH, C2'), 84.4 (CH, C3'), 68.0 (CH, C4'), 60.7 (CH, C1'), 34.7 (CH, C5'), 34.0 (CH_2 , C6'), 13.1 (CH_3 , C6). IR (cyclohexane): $\tilde{\nu}$ 2045.2 (90), 1977.7 (100), 1972.0 (80) cm^{-1} ($\text{C}\equiv\text{O}$). IR (film): $\tilde{\nu}$ 3462.3, 3419.6, br, 3376.4 , br cm^{-1} (N-H). MS (70 eV, EI): m/z (%): 375 (14) $[\text{M}]^+$, 319 (21), 289 (100), 233 (37), 213 (64), 157 (58), 134 (17). Anal. Calcd (%) for $\text{C}_{20}\text{H}_{17}\text{NO}_3\text{Fe}$ (375.2): C 64.02, H 4.57, N 3.73. Found: C 63.62, H 4.33, N 3.48.

14b and **14b'**. See above at the synthesis of **16e** for spectroscopic data.

2-tert-Butyl-5-methyl-3-propyl-1H-pyrrole (16d) and N-Ethyl-2,2-dimethylthiopropionimidic Acid Ethyl Ester (14a) (from 8e). Pentacarbonyl[1-(ethylthio)pentylidene]chromium (**8e**) (322 mg, 1.00 mmol), *N*-ethyl-2,2-dimethylpropionimidoyl chloride (**9a**) (295 mg, 2.00 mmol), and triethylamine (101 mg, 1.00 mmol) were reacted as described above to give compounds **16d** (146 mg, 82%) and **14a**.

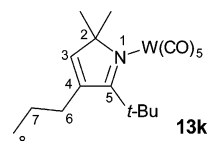
16d and **14a**. See above at the synthesis of **16d** for spectroscopic data.

5-Methyl-2-phenyl-3-propyl-1H-pyrrole (16e) and N-Ethylthiobenzimidic Acid Ethyl Ester (14b and 14b') (from 8e). Pentacarbonyl[1-(ethylthio)pentylidene]chromium (**8e**) (322 mg, 1.00 mmol), *N*-ethylbenzimidoyl chloride (**9b**) (335 mg, 2.00

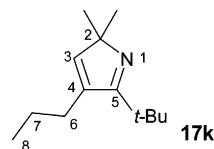
mmol), and triethylamine (101 mg, 1.00 mmol) were reacted as described above to give compounds **16e** (143 mg, 72%), **14b**, and **14b'**.

16e, **14b**, and **14b'**. See above at the synthesis of **16e** for spectroscopic data.

Pentacarbonyl[5-tert-butyl-2,2-dimethyl-4-propyl-2H-pyrrole-N]tungsten (13k), 5-tert-Butyl-2,2-dimethyl-4-propyl-2H-pyrrole (17k), and N-Isopropyl-2,2-dimethylthiopropionimidic Acid Ethyl Ester (14c). Pentacarbonyl[1-(ethylthio)pentylidene]tungsten (**8a**) (454 mg, 1.00 mmol), *N*-isopropyl-2,2-dimethylpropionimidoyl chloride (**9c**) (323 mg, 2.00 mmol), and triethylamine (101 mg, 1.00 mmol) were reacted as described above to give compounds **13k**, **17k**, and **14c**. They were not isolated, but characterized from ^1H and ^{13}C NMR spectra.



13k. ^1H NMR (300 MHz, CDCl_3 , $25\text{ }^\circ\text{C}$): δ 7.43 (t, br, $^4J = 1.7$ Hz, 1H; 3-H), 2.53 (dt, $^3J = 7.8$ and $^4J = 1.7$ Hz, 2H; 6- H_2), 1.71 (m, 2H; 7- H_2), 1.70 (s, 6H; 2 CH_3), 1.54 [s, 9H; $\text{C}(\text{CH}_3)_3$], 1.06 (t, $^3J = 7.3$ Hz, 3H; 8- H_3). ^{13}C NMR (CDCl_3 , $25\text{ }^\circ\text{C}$): 202.0 and 199.3 [C_q , 1:4 C; *trans*- and *cis*-CO of $\text{W}(\text{CO})_5$], 189.4 (C_q , C5), 161.9 (CH, C3), 138.5 (C_q , C4), 73.5 (C_q , C2), 37.3 [C_q , $\text{C}(\text{CH}_3)_3$], 29.7 (CH_2 , C6), 27.5 [$\text{C}(\text{CH}_3)_3$], 21.6 (2 CH_3), 21.5 (CH_2 , C7), 13.5 (CH_3 , C8).



17k. ^1H NMR (400 MHz, CDCl_3 , $25\text{ }^\circ\text{C}$): δ 6.81 (t, br, $^4J = 1.7$ Hz, 1H; 3-H), 2.38 (dt, $^3J = 7.7$ and $^4J = 1.7$ Hz, 2H; 6- H_2), 1.59 (m, 2H; 7- H_2), 1.28 [s, 9H; $\text{C}(\text{CH}_3)_3$], 1.23 (s, 6H; 2 CH_3), 0.99 (t, $^3J = 7.3$ Hz, 3H; 8- H_3). ^{13}C NMR (CDCl_3 , $25\text{ }^\circ\text{C}$): 179.2 (C_q , C5), 155.9 (CH, C3), 139.4 (C_q , C4), 73.6 (C_q , C2), 35.6 [C_q , $\text{C}(\text{CH}_3)_3$], 30.9 (CH_2 , C6), 28.5 [$\text{C}(\text{CH}_3)_3$], 23.6 (2 CH_3), 22.2 (CH_2 , C7), 14.1 (CH_3 , C8).

14c. ^1H NMR (300 MHz, CDCl_3 , $25\text{ }^\circ\text{C}$): δ 4.08 (sep, $^3J = 6.2$ Hz, 1H; NCH), 2.73 (q, $^3J = 7.5$ Hz, 2H; SCH_2), 1.25 (t, $^3J = 7.5$ Hz, 3H; SCH_2CH_3), 1.18 [s, 9H; $\text{C}(\text{CH}_3)_3$], 1.12 [d, $^3J = 6.2$ Hz, 6H; $\text{NCH}(\text{CH}_3)_2$].

Pentacarbonyl[5-tert-butyl-2,2,4-trimethyl-2H-pyrrole-N]tungsten (13l), 5-tert-Butyl-2,2,4-trimethyl-2H-pyrrole (17l), and N-Isopropyl-2,2-dimethylthiopropionimidic Acid Ethyl Ester (14c). Pentacarbonyl[1-(ethylthio)propylidene]tungsten (**8b**) (426 mg, 1.00 mmol), *N*-isopropyl-2,2-dimethylpropionimidoyl chloride (**9c**) (323 mg, 2.00 mmol), and triethylamine (101 mg, 1.00 mmol) were reacted as described above to give compounds **13l**, **17l**, and **14c**. They are not isolated but characterized from ^1H and ^{13}C NMR spectra.

13l. ^1H NMR (300 MHz, CDCl_3 , $25\text{ }^\circ\text{C}$): δ 7.49 (s, br, 1H; 3-H), 2.30 (s, 3H; 6- H_3), 1.70 (s, 6H; 2 CH_3), 1.54 [s, 9H; $\text{C}(\text{CH}_3)_3$]. ^{13}C NMR (CDCl_3 , $25\text{ }^\circ\text{C}$): 201.7 and 199.0 [C_q , 1:4 C; *trans*- and *cis*-CO of $\text{W}(\text{CO})_5$], 189.0 (C_q , C5), 163.6 (CH, C3), 133.1 (C_q , C4), 73.0 (C_q , C2), 36.8 [C_q , $\text{C}(\text{CH}_3)_3$], 27.1 [$\text{C}(\text{CH}_3)_3$], 21.4 (2 CH_3), 14.3 (CH_3 , C6).

17l. ^1H NMR (400 MHz, CDCl_3 , $25\text{ }^\circ\text{C}$): δ 6.86 (q, br, $^4J = 1.5$ Hz, 1H; 3-H), 2.12 (d, br, $^4J = 1.5$ Hz, 3H; 6- H_3), 1.32 [s, 9H; $\text{C}(\text{CH}_3)_3$], 1.29 (s, 6H; 2 CH_3). ^{13}C NMR (CDCl_3 , $25\text{ }^\circ\text{C}$): 180.5 (C_q , C5), 158.8 (CH, C3), 134.0 (C_q , C4), 73.3 (C_q , C2), 35.6 [C_q , $\text{C}(\text{CH}_3)_3$], 28.1 [$\text{C}(\text{CH}_3)_3$], 23.2 (2 CH_3), 15.0 (CH_3 , C6).

14c. See above at the synthesis of **13k** and **17k** for spectroscopic data.

***N*-Benzyl- α,α -*d*₂-benzimidoyl Chloride (*D*₂-**9e**).** To *N*-benzyl- α,α -*d*₂-benzamide (1.3 g, 6.1 mmol) in a 25 mL flask fitted with a reflux condenser was added thionyl chloride (0.80 g, 6.7 mmol) at room temperature. Then the reaction mixture was heated approximately 1 h at 100 °C after melting of the amide. After the reaction was completed, the flask was cooled to room temperature and the reaction mixture was washed with *n*-pentane. Finally, the solvent was removed under reduced pressure and the obtained imidoyl chloride *D*₂-**9e** was used directly without further purification (1.1 g, 79%, colorless liquid).

*D*₂-**9e**. ¹H NMR (300 MHz, CDCl₃, 25 °C): δ 8.05 and 7.33 (each m, 2:8 H; *o*-, *m*-, and *p*-H 2Ph). ¹³C NMR (CDCl₃, 25 °C): δ 143.4 (C_q, C=N), 138.0 and 135.6 (each C_q, each *i*-C Ph), 131.4, 129.1, 128.5, 128.3, 127.8, and 127.1 (each CH, *o*-, *m*-, and *p*-C 2Ph), 57.0 (quintet, CD₂). MS (70 eV, EI): *m/z* (%) 231 (0.2) [M]⁺, 196 (45) [M - Cl]⁺, 93 (100). Anal. Calcd (%) for C₁₄H₁₀D₂ClN (231.1): C 72.70, H 6.10, N 6.06. Found: C 72.35, H 5.88, N 6.27.

4-Deutero-2,5-diphenyl-3-propyl-1H-pyrrole ((4-*D*)-16e**).** Pentacarbonyl[1-(ethylthio)pentylidene]tungsten (**8a**) (123 mg, 0.27 mmol), *N*-benzyl- α,α -*d*₂-benzimidoyl chloride (*D*₂-**9e**) (125 mg, 0.54 mmol), and triethylamine (27 mg, 0.27 mmol) were heated as described above. After the removal of ether, the residue was washed with *n*-pentane (3 × 10 mL) and the solvent was removed again under reduced pressure. The immediate measurement of the ¹H NMR spectrum of the *n*-pentane-soluble part indicated the formation of pyrrole (4-*D*)-**16e**. On the other hand, pyrrole (4-*D*)-**16e**, *N*-benzyl- α,α -*d*₂-benzamide, and the triethylammonium salt were detected in the spectrum of the residue. The compound (4-*D*)-**16e** was analyzed from the latter spectrum. The compound was not purified further by chromatography in order to prevent proton exchange in the column.

(4-*D*)-**16e**. ¹H NMR (400 MHz, CDCl₃, 25 °C): δ 8.48 (s, br, 1H; NH), 2.63 (m, 2H; 6-H), 1.69 (m, 2H; 7-H), 0.99 (t, ³*J* = 7.3 Hz, 3H; 8-H).²⁴

Computational Details. All calculations were carried out with the density functional theory, DFT.²⁵ They employed the exchange functional of Becke²⁶ in conjunction with the correlation functional of Perdew²⁷ as well as the resolution of the identity (RI) approximation²⁸ for the fitting of the Coulomb potential (RI-BP86). The RI approximation largely increases the performance of pure DFT treatments without significantly decreasing accuracy. The geometries of the reactants, transition states (TS), and products were optimized with two basis sets denoted as BS1 and BS2 by using the Gaussian 03 program.²⁹ In BS1 the core electrons of sulfur and tungsten (small-core) were approximated by effective core potentials (ECP) of Hay and Wadt and the valence electrons described by the associated double- ζ basis.³⁰ For H, C, N, and O atoms an all-electron D95V basis set was used.³¹ The basis set BS1 is known by its acronym LANL2DZ. In BS2 the small-core electrons of tungsten were approximated by the quasi-relativistic ECP from the Stuttgart group³² and the valence electrons described by a TZVP basis: (7s6p5d)/[6s3p3d]. All-electron TZVP basis sets were used for the remaining atoms; S: (14s10p)/[5s5p], C, N, O: (11s6p1d)/[5s3p1d], H: (5s1p)/[3s1p]. The TZVP basis sets and ECP were taken from the TURBOMOLE basis set library³³ and introduced into Gaussian input with the Gen and Pseudo=read keywords. The auxiliary basis sets for the RI approximation were generated

(24) The phenyl signals in the ¹H NMR spectrum of the pyrrole (4-*D*)-**16e** overlap with the signals of *N*-benzyl- α,α -*d*₂-benzamide (at 7.53–7.19 ppm), which is generated by hydrolysis of the imidoyl chloride *D*₂-**9e**.

(25) (a) Parr, R. G.; Yang, W. *Density Functional Theory of Atoms and Molecules*; Oxford University Press: New York, 1989. (b) Koch, W.; Holthausen, M. C. *A Chemist's Guide to Density Functional Theory*; Wiley-VCH: Weinheim, 2000.

(26) Becke, A. D. *Phys. Rev. A* **1988**, *38*, 3098–3100.

(27) Perdew, J. P. *Phys. Rev. B* **1986**, *33*, 8822–8824.

(28) (a) Dunlap, B. I. *J. Chem. Phys.* **1983**, *78*, 3140–3142. (b) Eichkorn, K.; Treutler, O.; Öhm, H.; Häser, M.; Ahlrichs, R. *Chem. Phys. Lett.* **1995**, *242*, 652–660. (c) Treutler, O.; Ahlrichs, R. *J. Chem. Phys.* **1995**, *102*, 346–354. (d) Dunlap, B. I. *J. Mol. Struct. (THEOCHEM)* **2000**, *529*, 37–40. (e) Dunlap, B. I. *Phys. Chem. Chem. Phys.* **2000**, *2*, 2113–2116.

automatically according to the procedure implemented in Gaussian 03. The TSs were located with the QST3 procedure in which in addition to the structures of the specific reactant and product an initial TS structure is required as input.³⁴ The initial TS structures were located with the help of constrained geometry optimizations by freezing the appropriate reaction coordinate. All optimized structures correspond to fully converged geometries with gradients and displacements below the thresholds implemented in the Gaussian 03 program. The geometry optimizations of the reactants, transition states, and products were followed by vibrational frequency analyses. Harmonic frequencies were computed analytically and used without scaling. Reaction enthalpies ΔH were calculated from the differences between the total electronic energies (E_{elec}), zero-point-vibrational-energies (ZPVE), and thermal energies (E_{th}) of the products or TS with respect to the reactants and corrected for the volume work [$\Delta(PV)$] term (eq 1).³⁵

$$\Delta H = \Delta E_{\text{elec}} + \Delta \text{ZPVE} + \Delta E_{\text{th}} + \Delta(PV) \quad (1)$$

The thermal energy contributions (E_{th}) correspond to the sum of the changes in translational, rotational, and vibrational energies when going from 0 to 298.15 K. For the volume work term we assume ideal gas behavior, and thus it is equal to ΔnRT .³⁵

Acknowledgment. I.H.-K. thanks the SFB 424 (“Molekulare Orientierung als Funktionskriterium in Chemischen Systemen”) for financial support and Dr. Christian Mück-Lichtenfeld for technical support.

Supporting Information Available: (a) Selected optimized parameters and number of imaginary frequencies of the stationary structures for the MDPM rearrangement and the α -cyclization reactions calculated with the TZVP (Tables S1 and S3) and the LANL2DZ basis sets (Table S2); (b) BP86/LANL2DZ potential energy profiles for the MDPM rearrangements of the oxo and thio complexes; (c) BP86/LANL2DZ potential energy profiles for the hydride migration in **10h** and **11o**; (d) BP86/TZVP potential energy profile for the hydrogen transfer in **15m** to give **19m**. This material is available free of charge via the Internet at <http://pubs.acs.org>. OM700391T

(29) Frisch, M. J.; Trucks, G. W.; Schlegel, H. B.; Scuseria, G. E.; Robb, M. A.; Cheeseman, J. R.; Montgomery, J. A., Jr.; Vreven, T.; Kudin, K. N.; Burant, J. C.; Millam, J. M.; Iyengar, S. S.; Tomasi, J.; Barone, V.; Mennucci, B.; Cossi, M.; Scalmani, G.; Rega, N.; Petersson, G. A.; Nakatsuji, H.; Hada, M.; Ehara, M.; Toyota, K.; Fukuda, R.; Hasegawa, J.; Ishida, M.; Nakajima, T.; Honda, Y.; Kitao, O.; Nakai, H.; Klene, M.; Li, X.; Knox, J. E.; Hratchian, H. P.; Cross, J. B.; Adamo, C.; Jaramillo, J.; Gomperts, R.; Stratmann, R. E.; Yazyev, O.; Austin, A. J.; Cammi, R.; Pomelli, C.; Ochterski, J. W.; Ayala, P. Y.; Morokuma, K.; Voth, G. A.; Salvador, P.; Dannenberg, J. J.; Zakrzewski, V. G.; Dapprich, S.; Daniels, A. D.; Strain, M. C.; Farkas, O.; Malick, D. K.; Rabuck, A. D.; Raghavachari, K.; Foresman, J. B.; Ortiz, J. V.; Cui, Q.; Baboul, A. G.; Clifford, S.; Cioslowski, J.; Stefanov, B. B.; Liu, G.; Liashenko, A.; Piskorz, P.; Komaromi, I.; Martin, R. L.; Fox, D. J.; Keith, T.; Al-Laham, M. A.; Peng, C. Y.; Nanayakkara, A.; Challacombe, M.; Gill, P. M. W.; Johnson, B.; Chen, W.; Wong, M. W.; Gonzales, C.; Pople, J. A. *Gaussian 03 Rev. C01*; Gaussian, Inc.: Wallingford, CT, 2004.

(30) (a) Wadt, W. R.; Hay, P. J. *J. Chem. Phys.* **1985**, *82*, 284–298. (b) Hay, P. J.; Wadt, W. R. *J. Chem. Phys.* **1985**, *82*, 299–310.

(31) Dunning, T. H., Jr.; Hay, P. J. In *Modern Theoretical Chemistry*; Schaefer, H. F., III, Ed.; Plenum: New York, 1976; Vol. 3, pp 1–28.

(32) Andrae, D.; Häussermann, U.; Dolg, M.; Stoll, H.; Preuss, H. *Theor. Chim. Acta* **1990**, *77*, 123–141.

(33) The basis sets are available from the TURBOMOLE homepage <http://www.turbomole.com> via the FTP Server Button in the subdirectory basen.

(34) (a) Peng, C.; Schlegel, H. B. *Isr. J. Chem.* **1994**, *33*, 449–454. (b) Peng, C.; Ayala, P. Y.; Schlegel, H. B.; Frisch, M. J. *J. Comput. Chem.* **1996**, *17*, 49–56.

(35) (a) Del Bene, J. E. In *Molecular Structure and Energetics: Bonding Models*; Liebmann, J. F., Greenberg, A., Eds.; VCH: Deerfield Beach, FL, 1986; Vol. 1, pp 319–348. (b) Pitzer, K. S. *Quantum Chemistry*; Prentice Hall: Englewood Cliffs, NJ, 1961.